Supplementary Information for

# ATP-Fueled Autonomous Pathway-Selective Signal Transduction on DNA-Nanostructure Tracks

Xingyu Liu[1,2,3], Yan Liu[1,2,3], and Jie Deng[1,2,3]*

1. School of Chemistry and Chemical Engineering, Huazhong University of Science and Technology (HUST), Wuhan, China.

2. Hubei Key Laboratory of Bioinorganic Chemistry and Materia Medica, HUST, Wuhan, China.

3. Hubei Engineering Research Center for Biomaterials and Medical Protective Materials, HUST, Wuhan, China.

*Corresponding author. Email: jie_deng@hust.edu.cn

## Supplemental Materials and Methods

### Materials

All oligonucleotides were supplied by Integrated DNA Technologies Inc. (IDT) or Sangon Biotech (SG), and the sequences are shown in Supplementary Table. The biotinylated DNA strands and the 5'-phosphorylated DNA strands were ordered with HPLC purification, and all the other DNA strands were ordered with standard desalting purification. T4 DNA ligase (HC, 400 units (U) $\mu L^{-1}$, recombinant *E. coli* strain, *NEB* #M0202L), Nb.BtsI (10 U $\mu L^{-1}$, *NEB* #R0707S), and ATP solution (100 mM in 1 mM Tris-HCl, pH 7.5) were ordered from New England Biolabs (*NEB*). Acry/Bis 40% solution (19:1), agarose low EEO, formamide (deionized), urea (molecular biology grade), and GelRed nucleic acid gel stain were supplied by Sangon Biotech. Pierce™ streptavidin coated magnetic particles were supplied by Thermo Fisher Scientific. Ethylenediaminetetraacetic acid disodium salt dihydrate (EDTA, biology grade) was supplied by Acclea. Sodium chloride (NaCl, 99%), ammonium persulfate (APS, 98%), uranyl acetate, polyethylene glycol (PEG, average $M_n$=8000), DNA ladders (B598084, D598085), and glycerol were supplied by Aladdin Scientific. Ethylenediaminetetraacetic acid (EDTA, 99.5%), hexadecane (99%), Tris base (molecular biology grade), N,N,N',N'-tetramethyl ethylenediamine (TEMED, 98%), bromophenol blue, bovine serum albumin (Australia origin, low lgG, low fatty acid) and boric acid were supplied by J&K Scientific. xylene cyanol FF was supplied by TCI. Black 384-well microplate was ordered from Beijing Labgic Technology Co,Ltd. FCF400-CU-50 TEM grids were supplied by Zhongjingkeyi Films Technology Co., Ltd. Magnesium chloride hexahydrate ($MgCl_2$, 99% or 99.99%) was ordered from Sigma-Aldrich. 1.5 mm mini gel cassettes were purchased from Tanon.

### Instrumentation

Tanon MINI Space 3000 multifunctional gel image analysis system, vertical and horizontal gel electrophoresis systems (Tanon), gel electrophoresis power supplies (Tanon), EVOS M5000 Imaging System (ThermoFisher Scientific), Thermal Cycler (Analytik Jena), Refrigerated Centrifuge (Eppendorf 5425R), Nanodrop 2000 UV–Vis spectrophotometer (Thermo Fisher Scientific), Transmission Electron Microscopy (TEM) (HITACHI–HT7700), BioTek Synergy H1 Microplate Reader (Agilent).

### Buffer compositions

T4 DNA ligase storage buffer (*NEB*): 10 mM Tris-HCl (pH 7.4 at 25 °C), 50 mM KCl, 1 mM dithiothreitol (DTT), 0.1 mM EDTA, 50% glycerol.

Nb.BtsI storage buffer (*NEB*): 10 mM Tris-HCl (pH 7.4 at 25 °C), 50 mM NaCl, 1 mM DTT, 0.1 mM EDTA, 200 µg/ml BSA, 50% glycerol.

*NEB* rCutSmart® Buffer: 50 mM potassium acetate, 20 mM Tris-acetate, 10 mM magnesium acetate, 100 µg/ml recombinant albumin.

1× T4 DNA ligation buffer: 50 mM Tris-HCl (pH 7.4 at 25 °C), 10 mM $MgCl_2$, 1 mM ATP, 10 mM DTT

10× TBE buffer (1 L): 108 g Tris base, 55 g boric acid, and 5.84 g disodium EDTA.

10× TEF buffer: 50 mM Tris base, and 10 mM EDTA acid (n.b. results in pH 8.0 at 25 °C when mixed at this ratio, without any need for further acid/base titration).

Agarose gel loading buffer (AGLB): 30% glycerol, 0.025% xylene cyanol, 0.025% bromophenol blue.
Annealing Buffer: 1× TEF buffer, 50 mM NaCl.
Formamide loading buffer (FLB, 50 mL): 47.5 mL deionized formamide, 12.5 mg bromophenol blue, 2.5 mg xylene cyanol FF, 500 μL 0.5 M EDTA disodium salt (pH 8.0).
Washing buffer: 1× TEF supplemented with 12 mM $MgCl_2$ and 0.5% BSA.
Milli-Q water was used throughout of this study.

**Page purification (PAGE)**

The unpurified DNA strands with a length longer than 50 nucleotides (nt) were purified by denaturing polyacrylamide gel electrophoresis (dPAGE). Briefly, 15 wt.% dPAGE gels were prepared in empty 1.5 mm mini-gel cassettes. The oligonucleotides ordered at ca. 5 nmole scale were rehydrated with 50 μL of Milli-Q water, and mixed with equivalent volume of FLB. Samples were then loaded onto the dPAGE gel, with ca. 2–3 nmole per lane, followed by running the gel at 300 V for ca. 1 h in 0.5× TBE buffer, usually until the bromophenol blue dyes had run off the gel. Afterwards, the gel was wrapped in cling film and then placed on the TCL plate. The gel bands were identified by shadowing with UV light, marked using a marker pen, and then excised with a razor blade. An individual gel slice (no more than three lanes) was placed into a 2 mL round-bottom Eppendorf tube and crushed using a pestle, followed by adding 500 μL 1× TEF buffer. After shaking overnight at 37 °C and 1500 rpm, the mixture was transferred to a Freeze N' Squeeze spin column (Sangon Biotech) and spun at 10k rpm for 15–20 min. The filter containing waste acrylamide was then discarded, and 3 volumes of 100% ethanol that had been pre-cooled at -20 °C, along with 1/10 volume of 3 M NaCl, were then added to the Freeze N' Squeeze tube. The tube was then inverted several times to ensure thorough mixing of the contents. Afterwards, the tubes of different oligonucleotides were placed into a pre-cooled centrifuge (at ca. -6 °C), and spun at 20k rcf for 30 min, followed by removing the supernatant. The resulting pellets were washed twice with 75% ethanol using the centrifuge, with each spin lasting 15 min. The pellets were then dried at room temperature for ca. 20 mins, followed by rehydrating with 15–20 μL Milli-Q water. The concentration was then determined by a Nanodrop 2000c UV–Vis spectrophotometer.

**Agarose gel electrophoresis (AGE)**

2 wt.% agarose gel was prepared in 0.5× TBE buffer containing 12 mM $MgCl_2$ with a volume of ca. 100 mL, which was pre-stained with 3 μL GelRed (10,000× concentrate in $H_2O$) after the molten agarose was cooled to ca. 65 °C. Usually, 2–3 μL each reaction mixture was taken and mixed with 5 μL AGLB, and the mixed samples were then loaded onto the agarose gel. During the preparation and running processes of AGEs, dye bleaching was minimized by covering the gels with aluminum foil. All the agarose gels in this study were run at 85 V for 2–3 h in 0.5× TBE buffer containing 12 mM $MgCl_2$, followed by recording using a Tanon MINI Space 3000 multifunctional gel image analysis system. The obtained pictures were then proceeded with ImageJ.

**TEM measurements**

The structures were visualized through TEM by applying a negative stain to the samples. TEM grids were first cleaned using plasma discharge for 25 s, followed by placing 4 μL of the reaction mixture to the grid (for samples from dual-pathway nanostructure track, a 10-fold dilution was applied). After 2 min, the solution was wicked from the grid by gently touching filter paper to the grid edge. 4 μL of uranyl formate solution (2% w/v in $H_2O$, filtered through a 0.22 μm pore size membrane) was then placed onto the grid and the excess solution was immediately wicked using filter paper. The images were captured on a HITACHI-HT7700 TEM in brightfield mode at 100 kV.

**Structure stability characterization after nicking restriction**

To test the structural stability after nicking restriction, we further design a multi-stranded DNA nanostructure that can replicate the repeating unit of the cHCR (Supplementary Fig. 3A), and used FRET to monitor the integrity of the structure after nicking restriction. The experiments were performed in 1× *NEB* rCutSmart buffer at 37 and 25 °C containing 1 μM DNA nanostructure, and 1 U $\mu L^{-1}$ Nb.BtsI. The results were recorded by a microplate reader (Supplementary Fig. 3).

**Six-helix bundle DNA origami folding**

The experiments were performed in 1× TEF containing 12 mM $MgCl_2$, 10 or 40 nM M13 bacteriophage-derived "p7249", and 10- or 5-folds staple strands, followed by annealing via a 6025-thermal ramp (80 °C for 15 min, then at 60 °C for 5 min followed by its cooling to 25 °C over ca. 18 h). After the origami folding, 100 nM hairpin docking strand, 250 nM receptor hairpin and reporter, and 250 nM signal propagation units were added to assemble the four-station nanotrack scaffolded by p7249, and the reaction was carried out at 48 °C for overnight. For the fabrication of ten-station nanotrack, the conditions are the same as above except that 1 μM signal propagation units were used.

**ATP-fueled cHCR on the colloidal surface**

The experiments were performed in 1× *NEB* rCutSmart buffer at 25 °C containing 5 μM H3, 10 μM H2, 10 μM H4, 80 U $\mu L^{-1}$ T4 DNA ligase, 3 U $\mu L^{-1}$ Nb.BtsI, ca. $5.3\times10^5$ beads/mL colloids, and 5 μM ATP. Afterwards, the system was repeatedly fueled by adding another 5 μM ATP. At different time intervals (0 min, 8 h, 2 D, 3 D, 3.33 D, 4 D, 5 D, and 6 D), 1 μL aliquots of the suspension were taken. The colloids were collected by a magnet, washed with washing buffer for 5 times, and then resuspended in 5 μL 1× washing buffer. Then, the colloids were characterized by an inverted fluorescence microscopy under the same microscopy settings for quantification. ImageJ was used to measure the fluorescent intensities of the shells formed by DNA polymerization on the colloidal surfaces.

**Purification of DNA-nanostructure track**

The folded nanotracks were purified either by magnetic beads or by PEG precipitation. 30 μL of Pierce™ streptavidin coated magnetic beads (10 mg $mL^{-1}$) were washed with 100 μL 1× TEF with 16 mM $MgCl_2$ for 5 times. Afterwards, the particles were resuspended in 100 μL 1× TEF with 16 mM $MgCl_2$ and 1 μM biotinylated DNA strands that can capture the folded nanotracks, and the

reaction was carried out at 4 °C for overnight. The particles were then washed using the same buffer for 5 times. Then, 200 μL of the folded nanostructures were mixed with the functionalized magnetic beads. After incubating at room temperature for 30 min, the magnetic beads were transferred into 50 μL elution buffer (1× TEF, 16 mM $MgCl_2$, 1 μM invading DNA strands) and reacted at room temperature for 30 min, and the released magnetic beads were washed with 100 μL 1× TEF containing 16 mM $MgCl_2$ for 5 times before transferring back to the solution containing uncaptured DNA nanostructures. This process was repeated for 3 times to ensure maximum yield of the purified products. Additionally, PEG precipitation was used for large-scale preparation of the purified nanotracks. Briefly, a certain amount of 1 M $MgCl_2$ was added to the folded structures to reach a final $MgCl_2$ concentration of 20 mM. Then, equal volume of 2× PEG-purification buffer (1× TEF, 15 wt.% PEG-8000, 510 mM NaCl) was added and mixed with the origami solution. The mixture was spun at 20,000 rcf for 25 min. The supernatant was gently extracted using a pipette and the pellet was resuspended in 100 μl 1× TEF with 20 mM $MgCl_2$. The second round of PEG precipitation was performed using an equal volume of 2× PEG-purification buffer and the final origami pellet was resuspended in a small volume of 1× TEF buffer containing 12 mM $MgCl_2$ for further use.

**ATP-fueled transient directional signal transduction on a four-station nanotrack with varied inter-hairpin distance**

The DNA nanostructure tracks with varied inter-hairpin distance were fabricated and purified the same as that for the standard four-station nanotrack. The signal transduction experiments were performed in 1× *NEB* rCutSmart buffer at 37 °C containing 50 nM DNA-nanostructure track with an inter-hairpin distance of 5, 7.5, or 10 nm, 500 nM quencher strand, 500 nM initiator, 80 U $\mu L^{-1}$ T4 DNA ligase, 0.1 U $\mu L^{-1}$ Nb.BtsI, and 1 μM ATP. The experiments were carried out in a total volume of ca. 20 μL in a black 384-well plate, and the results were recorded every 2 min by a plate reader with an excitation at 627 nm and an emission at 672 nm (20 nm for both bandwidths). Note: a layer of hexadecane (15 μL) was added on top of the reaction solution to prevent evaporation at 37 °C.

**ATP-dependent lifetime of fuel-driven transient directional signal transduction on a four-station nanotrack**

The experiments were carried out in 1× *NEB* rCutSmart buffer at 37 °C containing 50 nM DNA-nanostructure track supplemented with 500 nM quencher strand, 500 nM initiator, 80 U $\mu L^{-1}$ T4 DNA ligase, 0.1 U $\mu L^{-1}$ Nb.BtsI, and varied concentration of ATP (0, 0.2, 0.5, 1, and 2 μM). The experiments were carried out in a total volume of ca. 20 μL in a black 384-well plate, and the results were recorded every 2 min by a plate reader with an excitation at 627 nm and an emission at 672 nm (20 nm for both bandwidths). Note: a layer of hexadecane (15 μL) was added on top of the reaction solution to prevent evaporation at 37 °C.

**Comparison of fuel-driven directional signal transduction on a four-station nanotrack at 25 and 37 °C**

Fist, the reaction were performed without the presence of Nb.BtsI. The experiments were carried out at 25 and 37 °C in 1× *NEB* rCutSmart buffer containing 50 nM DNA-nanostructure track supplemented with 500 nM quencher strand, 500 nM initiator, 80 U $\mu L^{-1}$ T4 DNA ligase, and 1 μM ATP. The experiments were carried out in a total volume of ca. 20 μL in a black 384-well plate, and the results were recorded every 2 min by a plate reader with an excitation at 627 nm and an emission at 672 nm (20 nm for both bandwidths). Note: a layer of hexadecane (15 μL) was added on top of the reaction solution to prevent evaporation.

Then, with the presence of Nb.BtsI, the experiments were carried out at 25 and 37 °C in 1× *NEB* rCutSmart buffer containing 50 nM DNA-nanostructure track supplemented with 500 nM quencher strand, 500 nM initiator, 80 U $\mu L^{-1}$ T4 DNA ligase, 0.1 U $\mu L^{-1}$ Nb.BtsI and 1 μM ATP. The experiments were carried out in a total volume of ca. 20 μL in a black 384-well plate, and the results were recorded every 2 min by a plate reader with an excitation at 627 nm and an emission at 672 nm (20 nm for both bandwidths). Note: a layer of hexadecane (15 μL) was added on top of the reaction solution to prevent evaporation.

**The evaluation of stability of nicked intermediate product in the nanotrack**

Supplementary Fig. 16 presents the design of a three-station nanotrack, in which the signal receptor was engineered to either permit or prevent nicking restriction following ligation. The folding and purification of the nanostructures were carried out identically to those used for fabricating the DNA-nanostructure track. This setup enables further investigation into the degradation mechanisms of ATP-fueled transient signal transduction systems—specifically, whether degradation occurs via terminal monomer refolding and shedding, refolding from the initiating hairpin, or collapse at intermediate stages after nicking. The experiments were performed in 1× *NEB* rCutSmart buffer at 37 °C containing 50 nM DNA-nanostructure track supplemented with 500 nM quencher strand, 500 nM initiator, 80 U $\mu L^{-1}$ T4 DNA ligase, and 500 nM ATP. 0.2 U $\mu L^{-1}$ Nb.BtsI was added after reacting for 9 h. The experiments were carried out in a total volume of ca. 20 μL in a black 384-well plate, and the results were recorded every 2 min by a plate reader with an excitation at 627 nm and an emission at 672 nm (20 nm for both bandwidths). Note: a layer of hexadecane (15 μL) was added on top of the reaction solution to prevent evaporation.

**Characterization of potential inter-particle cross-interaction**

Supplementary Fig. 20 presents the design of two types of DNA-nanostructure tracks, each bearing a distinct FRET reporter pair. The signal propagating and reporting hairpins are identical, but one pair of FRET reporter-modified nanostructures was designed to either include or lack the receptor hairpin. The signaling from both FRET channels was then measured simultaneously after addition of the initiator. The DNA-nanostructure tracks were fabricated following the same procedure used for the preparation of the four-station nanotrack above. Afterwards, the experiments were performed in 1× *NEB* rCutSmart buffer at 37 °C containing 50 nM each of the two types of DNA-nanostructure tracks (each with a distinct FRET pair), 500 nM initiator, 80 U $\mu L^{-1}$ T4 DNA ligase, 0.1 U $\mu L^{-1}$ Nb.BtsI and 1 μM ATP. The experiments were carried out in a total volume of ca. 20 μL in a black 384-well plate, and the results were recorded every 2 min by a plate reader with an

excitation at 627 nm and an emission at 672 nm (20 nm for both bandwidths). Note: a layer of hexadecane (15 μL) was added on top of the reaction solution to prevent evaporation.

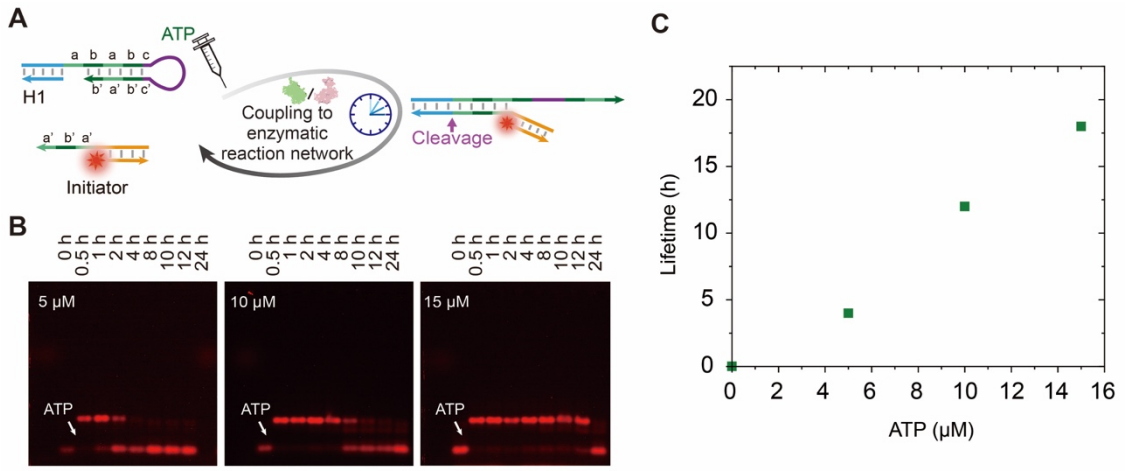


**Supplementary Fig. 1. ATP-fueled transient hairpin opening with programmable lifetimes govern by ATP concentration.** (**A**) Schematic illustration of ATP-driven transient hairpin opening. (**B**) Uncroped AGE images for those presented in Fig. 2B in main manuscript. (**C**) Lifetimes are controlled by the ATP concentration. Conditions: 1× *NEB* rCutSmart buffer at 25 °C containing 1 μM initiator, 2 μM hairpin, 40 U $\mu L^{-1}$ T4 DNA ligase, and 1 U $\mu L^{-1}$ Nb.BtsI. The red color in the scheme and gel images represent Cy5. The experiments in Supplementary Fig. 1B and C were independently repeated three times with similar results. Source data are provided as a Source Data file.

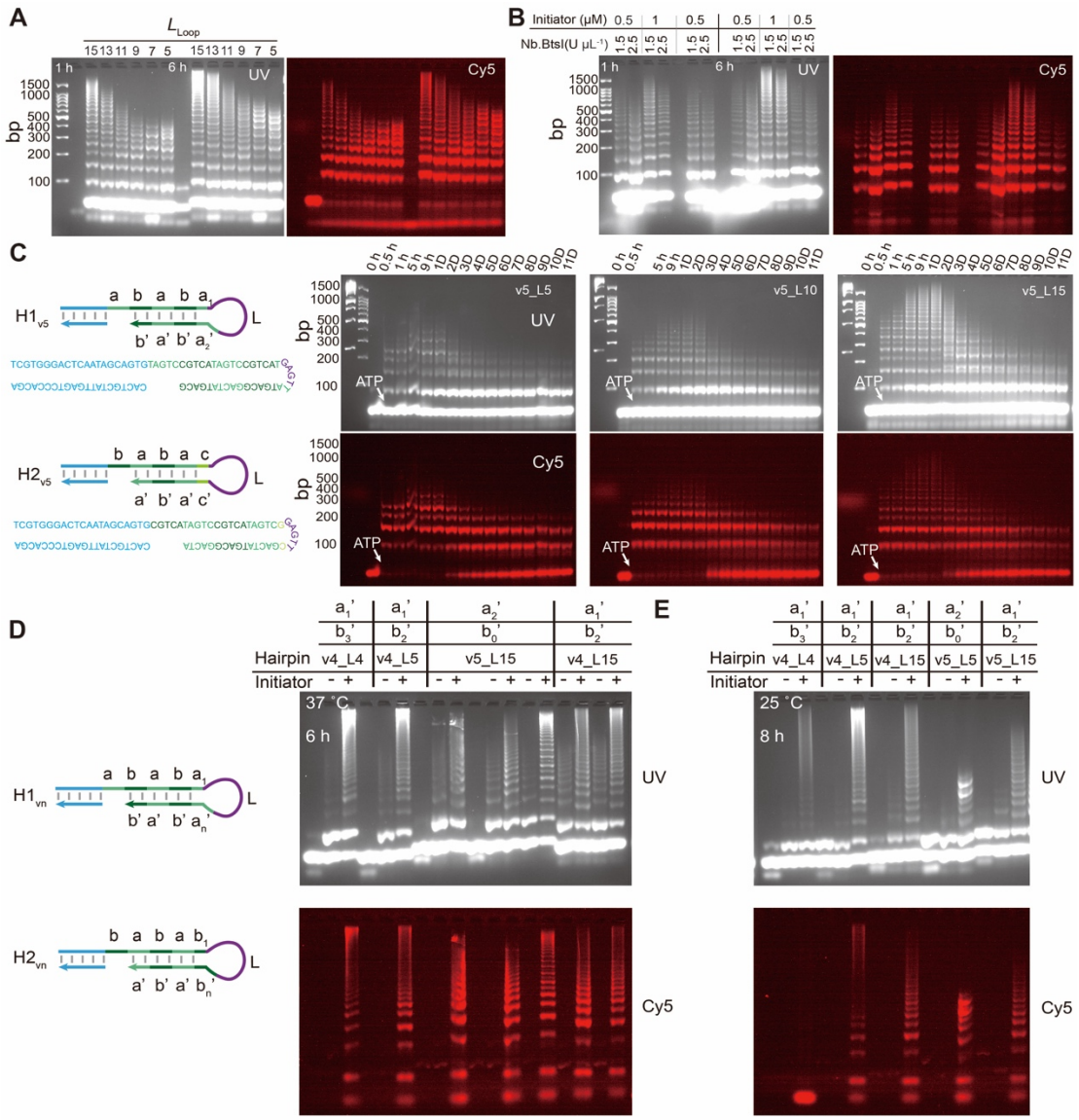


**Supplementary Fig. 2. ATP-fueled transient cHCRs using $H_{v5}$ and $H_{v4}$.** (A) AGE analyses of ATP-fueled transient cHCRs of $H_{v5}$ at varied loop lengths (2 wt. %, 85 V, 2 h). (B) AGE analyses of ATP-fueled transient cHCRs of $H_{v5}$ at varied concentrations of initiator and Nb.BtsI (2 wt. %, 85 V, 2 h). (C) AGE analyses of ATP-fueled transient cHCRs of $H_{v5}$ with varied loop lengths (5, 10, and 15 nt) (2 wt. %, 85 V, 2 h). (D,E) Comaprision of ATP-fueled transient cHCRs of $H_{v4}$ and $H_{v5}$ at varied loop lenghts at (D) 37 °C and (E) 25 °C, seen by AGE (2 wt. %, 85 V, 2 h). Conditions: (A) 1× T4 DNA ligation buffer, 37 °C, 1 μM initiator, 10 μM $H1_{v5\_L15}$, 10 μM $H2_{v5\_L15}$, 40 U $\mu L^{-1}$ T4 DNA ligase. (B) 1× *NEB* rCutSmart buffer, 37 °C, 0.5 or 1 μM initiator, 10 μM $H1_{v5}$, 10 μM $H2_{v5}$, 60 U $\mu L^{-1}$ T4 DNA ligase, 1.5 or 2.5 U $\mu L^{-1}$ Nb.BtsI, and 60 μM ATP. (C) 1× *NEB* rCutSmart buffer, 37 °C, 1 μM initiator, 10 μM $H1_{v5}$, 10 μM $H2_{v5}$, 60 U $\mu L^{-1}$ T4 DNA ligase, 2.5 U $\mu L^{-1}$ Nb.BtsI, and 40 μM ATP. (D, E) 1× T4 DNA ligation buffer, 1 μM initiator, 10 μM each hairpin monomer, 40 U $\mu L^{-1}$ T4 DNA ligase. The experiments in Supplementary Fig. 2A–E were independently repeated three times with similar results.

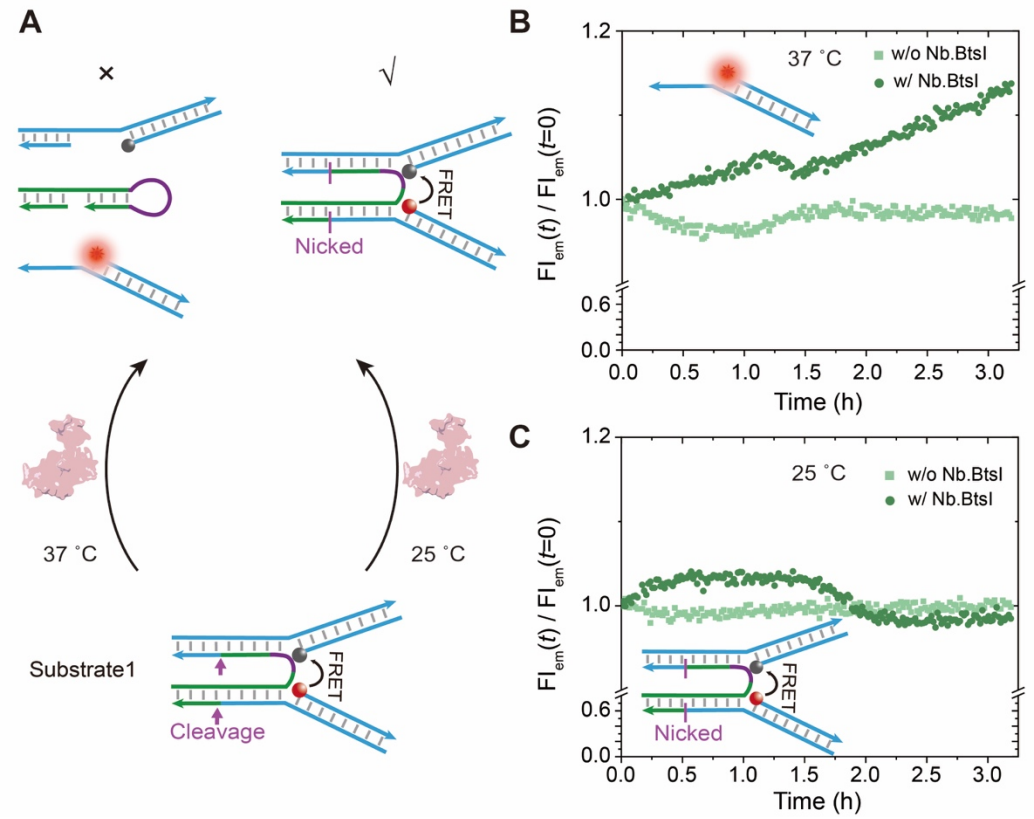


**Supplementary Fig. 3. The stability of intermediate product of ATP-fueled transient cHCR after nicking restriction.** (A) Schematic of structure degradation after nicking restriction at 37 and 25 °C. Time-dependent FI measurements of the degradation of the nicked structures at (B) 37 and (C) 25 °C. Conditions: 1× *NEB* rCutSmart buffer, 1 μM DNA nanostructure, and 1 U $\mu L^{-1}$ Nb.BtsI. Note: The FI for the nicked structure gradually increases over time at 37 °C, indicating its graudal dissociation, while there is no obvious FI increase for the nicked structure at 25 °C. This suggests that the nicked structure remains stable at 25 °C. Therefore, we assume that chain fragmentation is negligible for the ATP-fueled transient cHCR after nicking restriction at 25 °C. Red and black balls in the schemes represent Cy5 and dye quencher, respectively. The experiments in Supplementary Fig. 3B and C were independently repeated three times with similar results. Source data are provided as a Source Data file.

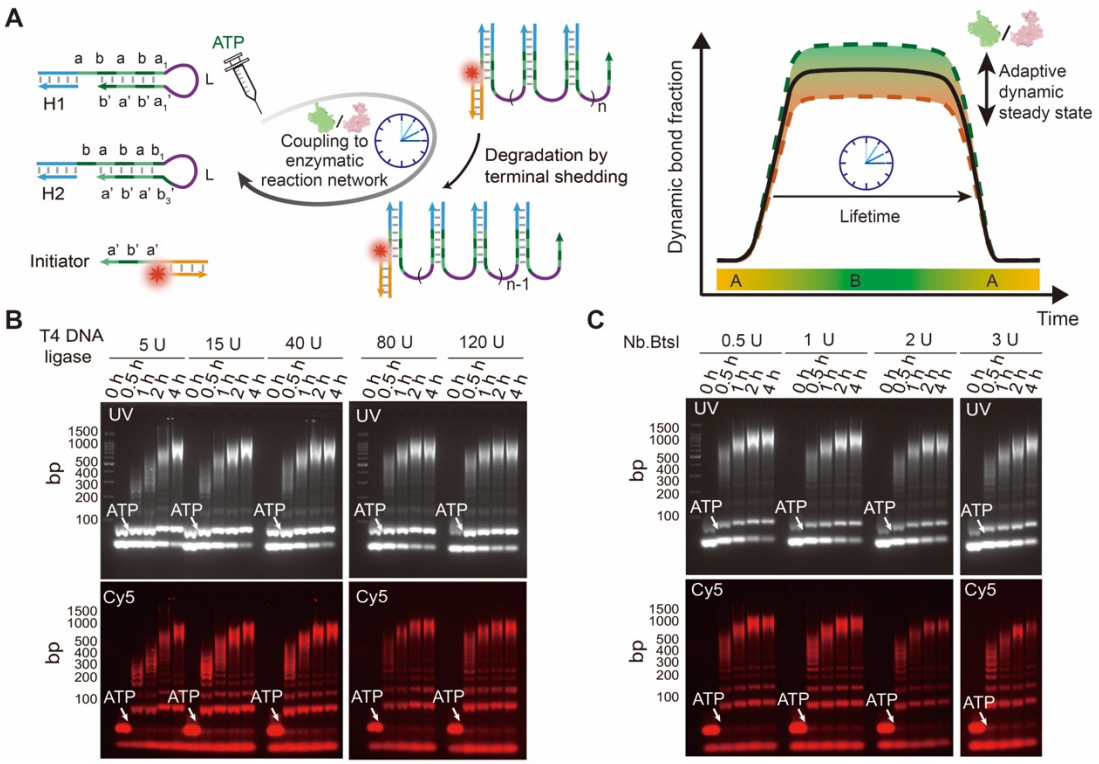


**Supplementary Fig. 4. Adaptive DySS of ATP-fueled transient cHCR regulated by the concentrations of both enzymes.** (A) Schematic illusraton of ATP-fueled transient cHCR with adaptive DySS. The red balls represent Cy5. (B) AGE analyses of ATP-fueled transient cHCR with varied cooncentration of T4 DNA ligase (2 wt. %, 85 V, 2 h). (C) AGE analyses of ATP-fueled transint cHCR with varied concentration of Nb.BtsI (2 wt. %, 85 V, 2 h). Conditions: (B) 25 °C, 40 μM ATP, 1 μM initiator, and 10 μM H1, 10 μM H2, and varied concenration of T4 DNA ligase (5, 15, 40, 80, and 120 U $\mu L^{-1}$). (C) The same as (B) but used 80 U $\mu L^{-1}$ T4 DNA ligase and varied concentration of Nb.BtsI (0.5, 1, 2, and 3 U $\mu L^{-1}$). The experiments in Supplementary Fig. 4B and C were independently repeated three times with similar results. Uncopped gel scans are supplied in Supplementary Fig. 25.

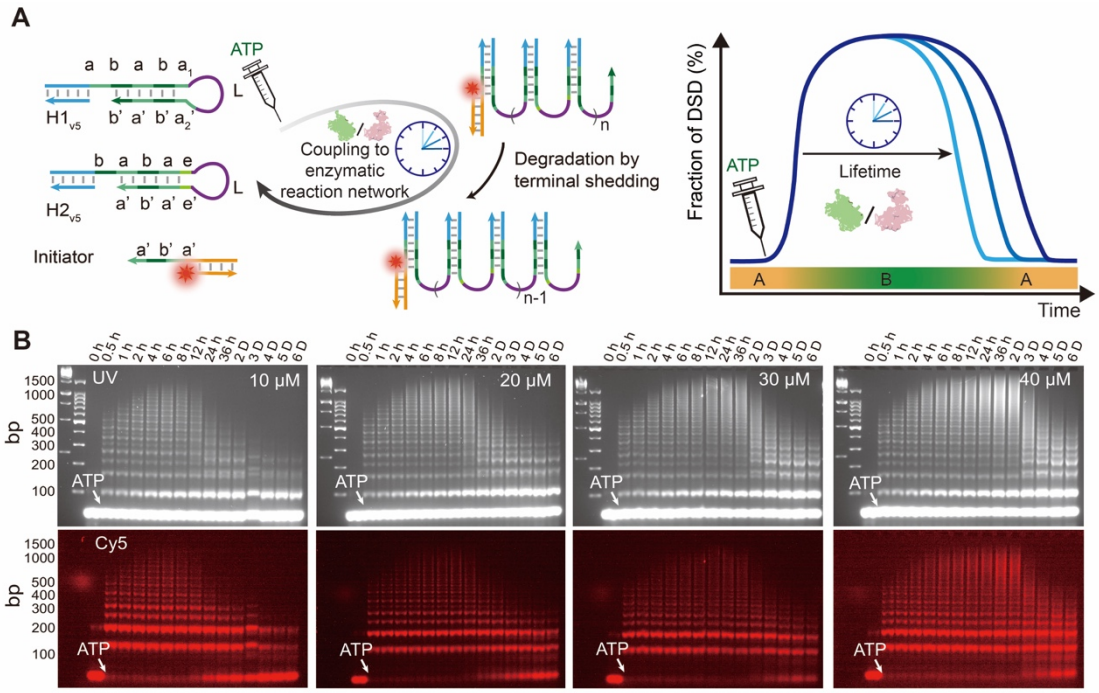


**Supplementary Fig. 5. ATP-fueled transient cHCR of $H_{v5}$ with programmable lifetimes govern by ATP oncentration.** (A) Schematic illustration of ATP-fueled transient cHCR. The red balls represent Cy5. (B) AGE analyses of time-dependent aliquots of ATP-fueled transient cHCR of $H_{v5}$ at varied concentration of ATP (2 wt. %, 85 V, 2 h). Conditions: 37 °C, 1 μM initiator, 10 μM each hairpin monomer, 60 U $\mu L^{-1}$ T4 DNA ligase, 2.5 U $\mu L^{-1}$ Nb.BtsI, and varied concentration of ATP (10, 20, 30, and 40 μM). The experiments in Supplementary Fig. 5B were independently repeated three times with similar results.

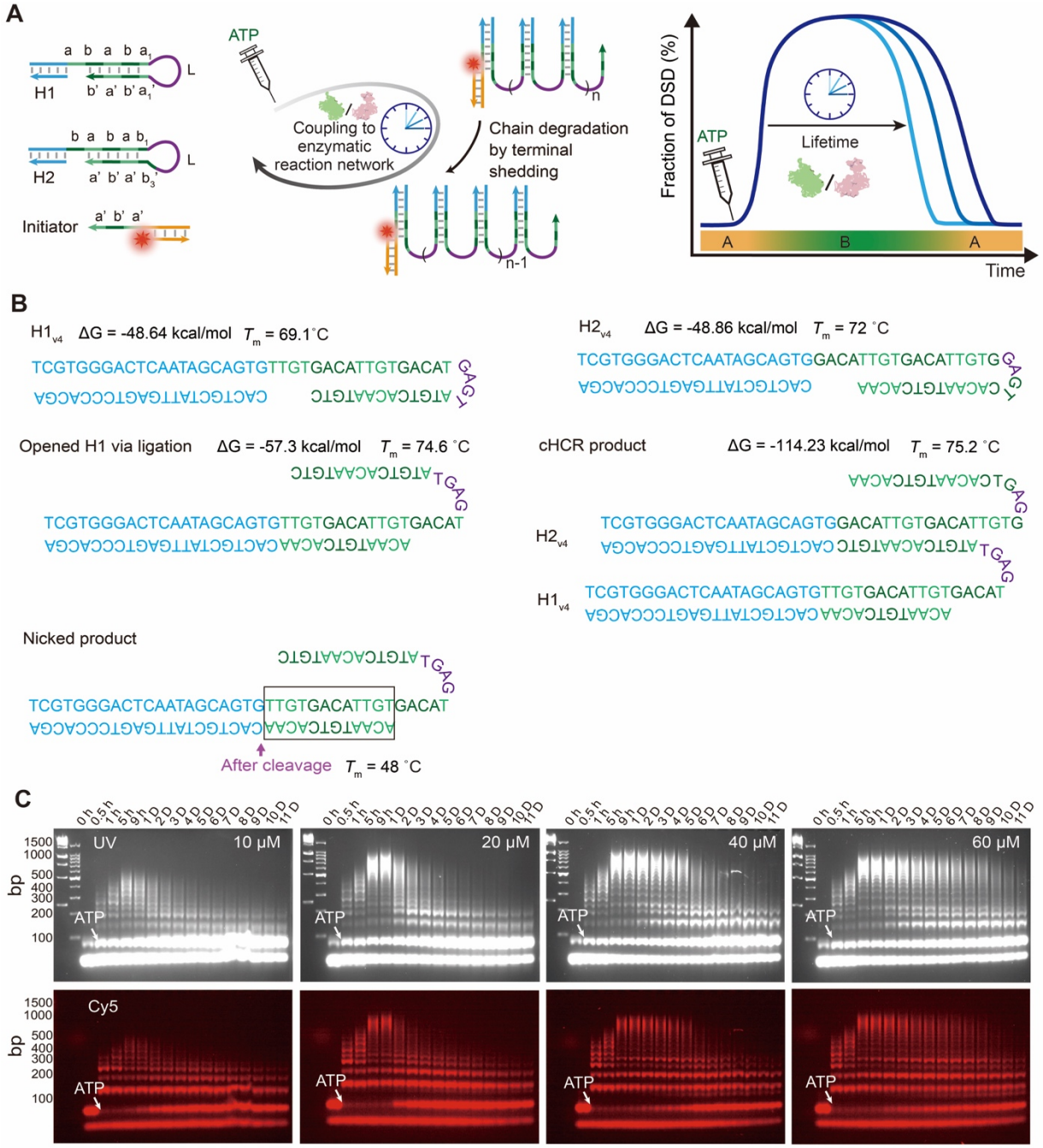


**Supplementary Fig. 6. ATP-fueled transient cHCR of $H_{v4}$ with programmable lifetimes govern by ATP oncentration.** (A) Schematic illustration of ATP-powered transient cHCR. The red balls represent Cy5. (B) thermodynamic parameters of the key components of the system, analyzed by NUPACK at 25 °C, 50 mM NaCl, 10 mM $MgCl_2$, and 1 μM each species. (C) AGE analyses of time-dependent aliquotsof ATP-fueled transient cHCR of $H_{v4}$ at varied ATP concentration (2 wt. %, 85V, 2 h). Conditions: 25 °C, 1 μM initiator, 10 μM each hairpin monomer, 80 U $\mu L^{-1}$ T4 DNA ligase, 3 U $\mu L^{-1}$ Nb.BtsI and varied concentration of ATP (10, 20, 40, and 60 μM). The experiments in Supplementary Fig. 6C were independently repeated three times with similar results.

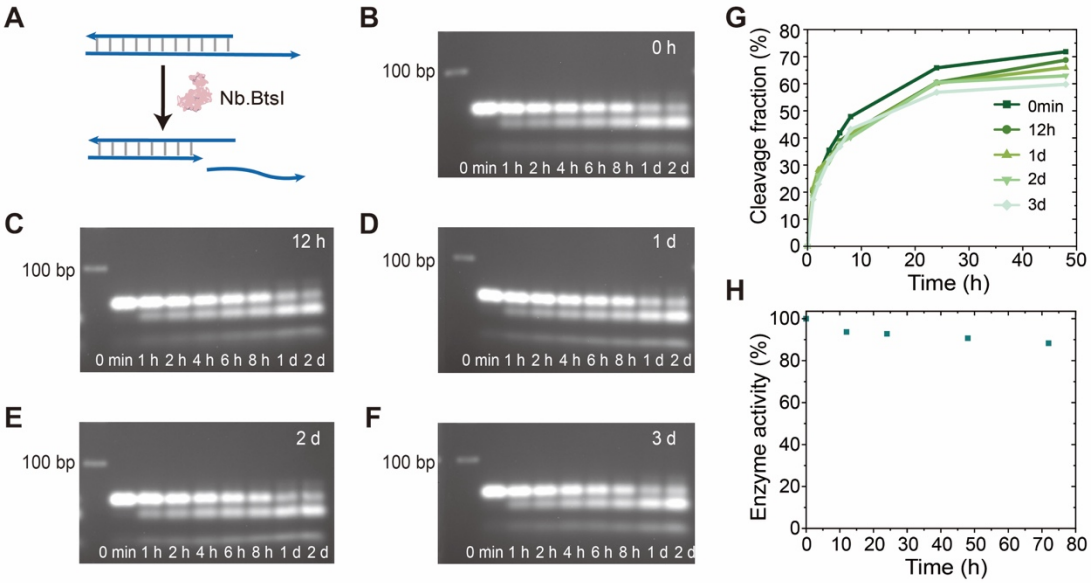


**Supplementary Fig. 7. Nb.BtsI activity and stability after pre-incubating at 37 °C for varied period of time.** (A) Schematic representation of the cleavage of dsDNA by Nb.BtsI. (B-F) Time-dependent AGE (2 wt. %, 85 V, 2 h) for the dsDNA cleavage by the Nb.BtsI with different pre-incubation times at 37 °C (B, 0 h; C, 12 h; D, 1 day; E, 2 days; F, 3 days). (G) Time-dependent fractions of dsDNA cleavage by the restriction enzyme with different time for pre-incubation. (H) Nb.BtsI activity after varied pre-incubation time. The line is a guide to the eye. Conditions: 37 °C, 1× *NEB* rCutSmart buffer, 0.01 mM dsDNA, and 1.5 U $\mu L^{-1}$ Nb.BtsI. The experiments in Supplementary Fig. 7B–F were independently repeated three times with similar results. Uncopped gel scans are supplied in Supplementary Fig. 26. Source data are provided as a Source Data file.

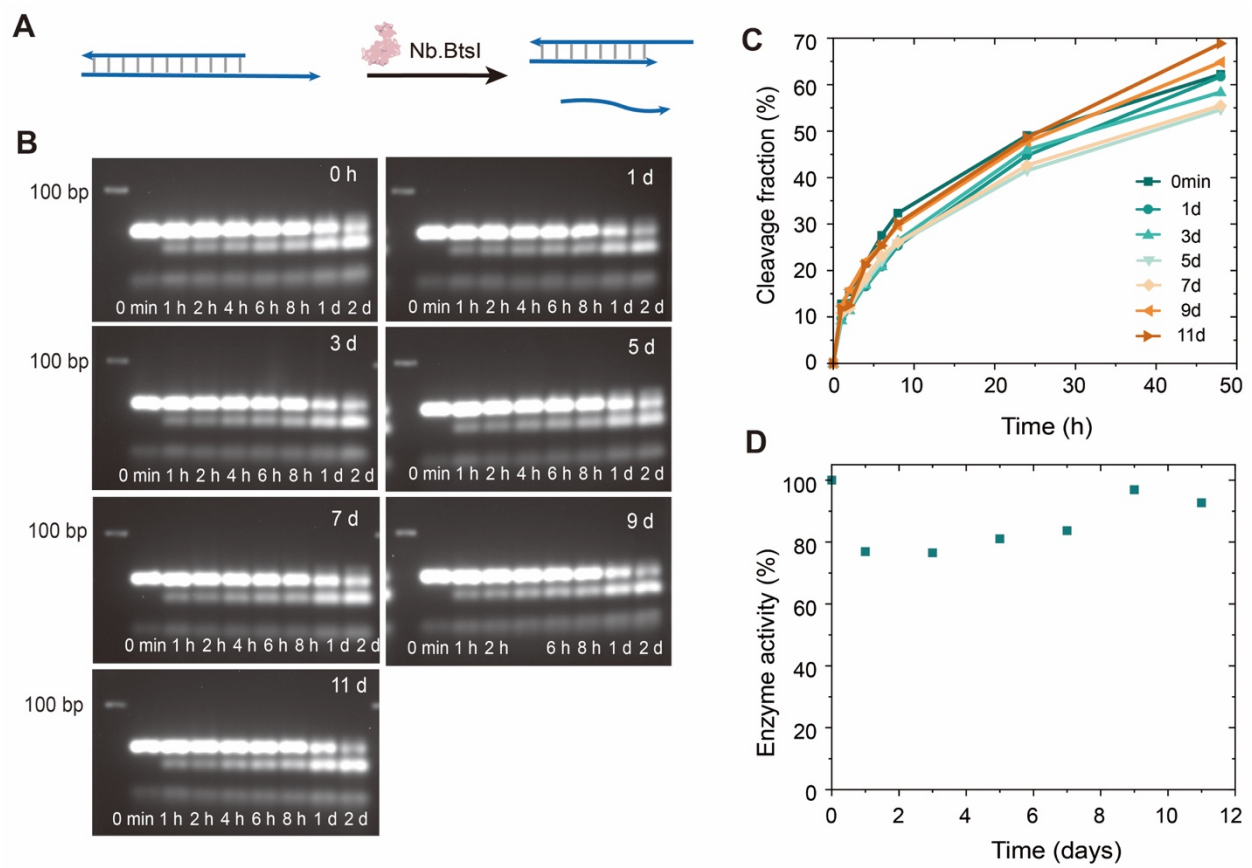


**Supplementary Fig. 8. Nb.BtsI activity and stability after pre-incubating at 25 °C for varying durations.** (A) Schematic representation of the cleavage of dsDNA by Nb.BtsI. (B) Time-dependent AGE (2 wt. %, 85 V, 2 h) for the dsDNA cleavage by the Nb.BtsI with different pre-incubation time at 25 °C (0 h, 1 day, 3 days, 5 days, 7 days, 9 days, and 11 days). (C) Time-dependent fractions of dsDNA cleavage by the restriction enzyme with varying durations of pre-incubation. (D) Nb.BtsI activity after varying pre-incubation durations. Conditions: 25 °C, 1× *NEB* rCutSmart buffer, 0.01 mM dsDNA, and 1.5 U $\mu L^{-1}$ Nb.BtsI. The experiments in Supplementary Fig. 8B were independently repeated three times with similar results. Uncopped gel scans are supplied in Supplementary Fig. 27. Source data are provided as a Source Data file.

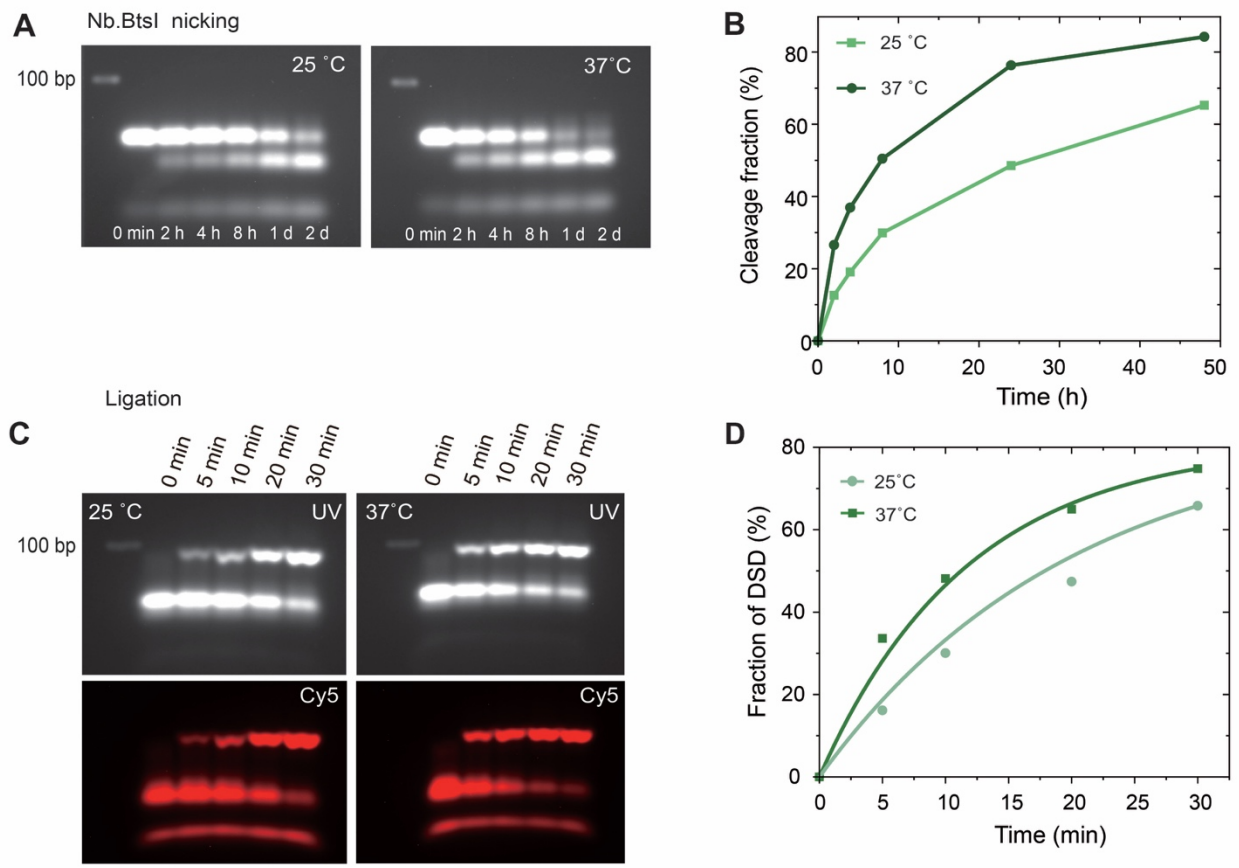


**Supplementary Fig. 9. Comparing enzyme activities of Nb.BtsI and T4 DNA ligase at 25 and 37 °C.** (A) Time-dependent AGE analyses of dsDNA cleavage by Nb.BtsI at 25 and 37 °C (2 wt. %, 85 V, 2 h). (B) Plotted cleavage fractions of dsDNA substrates quantified from the gel images in (A). Nb.BtsI at 25 °C was calculated to have ca. 56.4% activity compared to its activity at 37 °C. (C) Time-dependent AGE analyses of ATP-fueled ligation of a fluorescently labeled initiator to a hairpin (2 wt. %, 85 V, 2 h). (D) Plotted fraction of DSD via ligation at 25 and 37 °C, as quantified by the gel images in (C). T4 DNA ligase at 25 °C was calculated to have ca. 78.8% activity compared to its activity at 37 °C. Conditions: (A) 1× *NEB* rCutSmart buffer, 0.01 mM dsDNA, 1.5 U $\mu L^{-1}$ Nb.BtsI, and reacting at 25 and 37 °C. (C) 1× *NEB* rCutSmart buffer, 10 μM initiator, 10 μM hairpin, 5 U $\mu L^{-1}$ T4 DNA ligase, 100 μM ATP, and reacting at 25 and 37 °C. The experiments in Supplementary Fig. 9A and C were independently repeated three times with similar results. Uncopped gel scans are supplied in Supplementary Fig. 28. Source data are provided as a Source Data file.

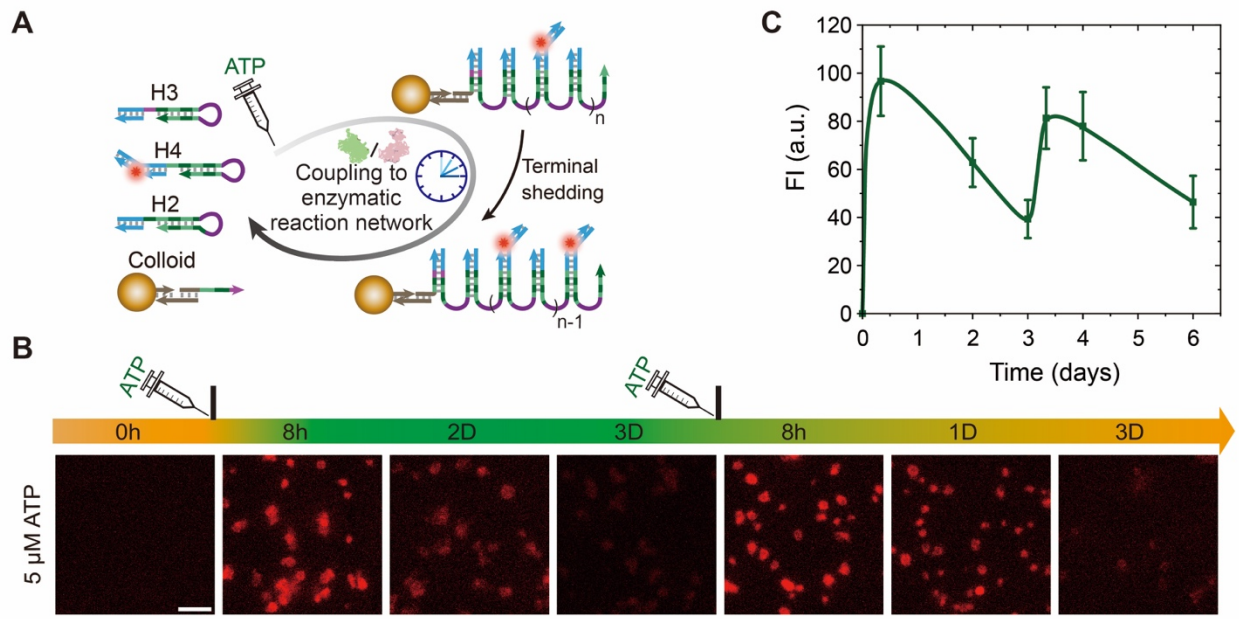


**Supplementary Fig. 10. Repeated fueling of transient cHCR on colloidal surfaces.** (A) Schematic illustration of ATP-fueled DNA polymerization on paramagnetic colloids. (B) Inverted fluorescence microscopy measurements of transient DNA polymerization on the colloidal surfaces with repeated fueling. Scale bar: 5 μm. (C) Time-dependent FIs of the colloids. The line is a guide to the eye. Error bars correspond to the mean ± SD ($N = 80$). Conditions: 1× *NEB* rCutSmart buffer, 25 °C, 5 μM H3, 10 μM H2, 10 μM H4, 80 U $\mu L^{-1}$ T4 DNA ligase, 3 U $\mu L^{-1}$ Nb.BtsI, and 5 μM ATP for both rounds of fueling. Red color in the scheme and fluorescence images represent Cy5. The experiments in Supplementary Fig. 10 B were independently repeated three times with similar results. Source data are provided as a Source Data file.

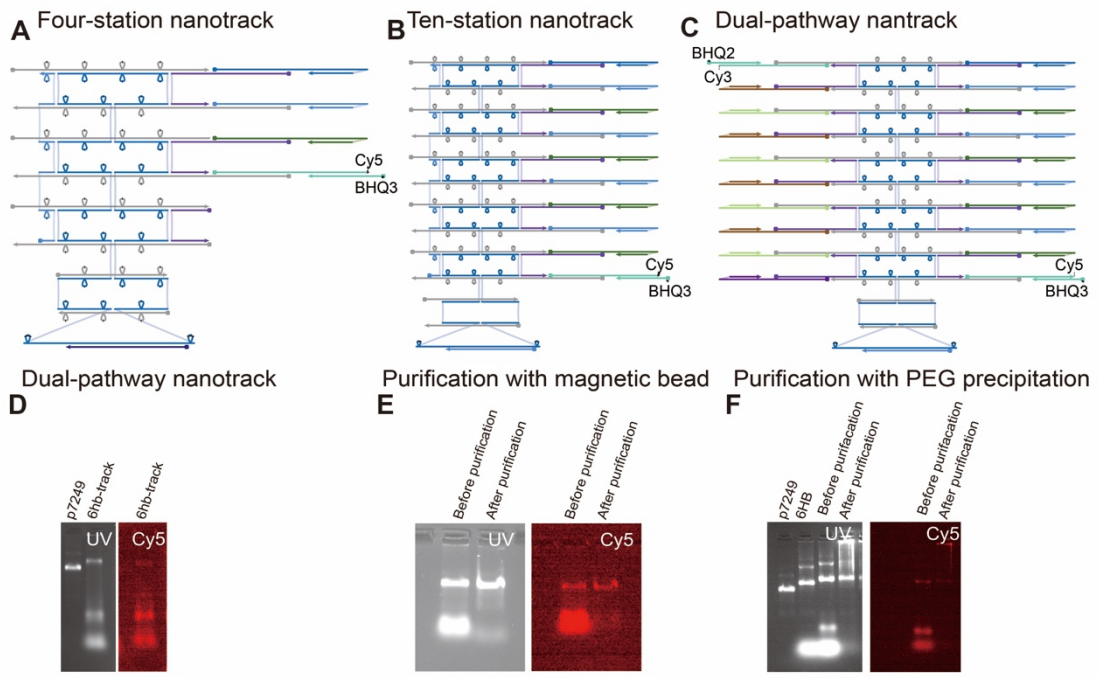


**Supplementary Fig. 11. DNA-nanostructure track.** (A) Design of a four-station DNA-nanostructure track. (B) Design of a ten-station DNA-nanostructure track. (C) Design of a dual-pathway DNA-nanostructure track. (D) AGE analyses of the dual-pathway DNA nanostructure track before and after folding (1 wt. %, 65 V, 2 h). (E, F) AGE analyses of the folded nanotracks after purification by magnetic beads or by PEG precipitation (1 wt. %, 65 V, 2 h). The experiments in Supplementary Fig. 11D–F were independently repeated three times with similar results.

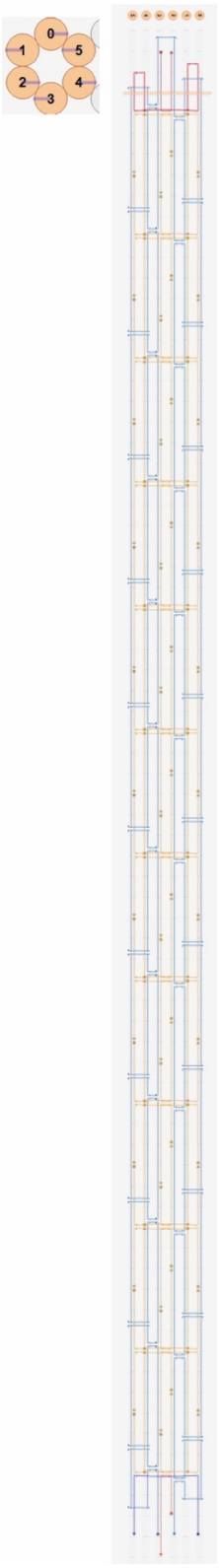


**Supplementary Fig. 12. Strand rooting diagram for 6HB origami.**

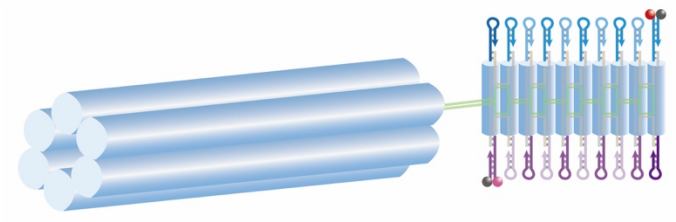

**Supplementary Fig. 13. Schematic of a dual-pathway nanostructure track adjacent to a six-helix bundle DNA origami.** To facilitate large-scale preparation of the nanostructures via PEG precipitation, a six-helix bundle DNA origami is folded adjacent to the nanotrack. Red, magenta, and black balls in the schemes represent Cy5, Cy3, and dye quencher, respectively.

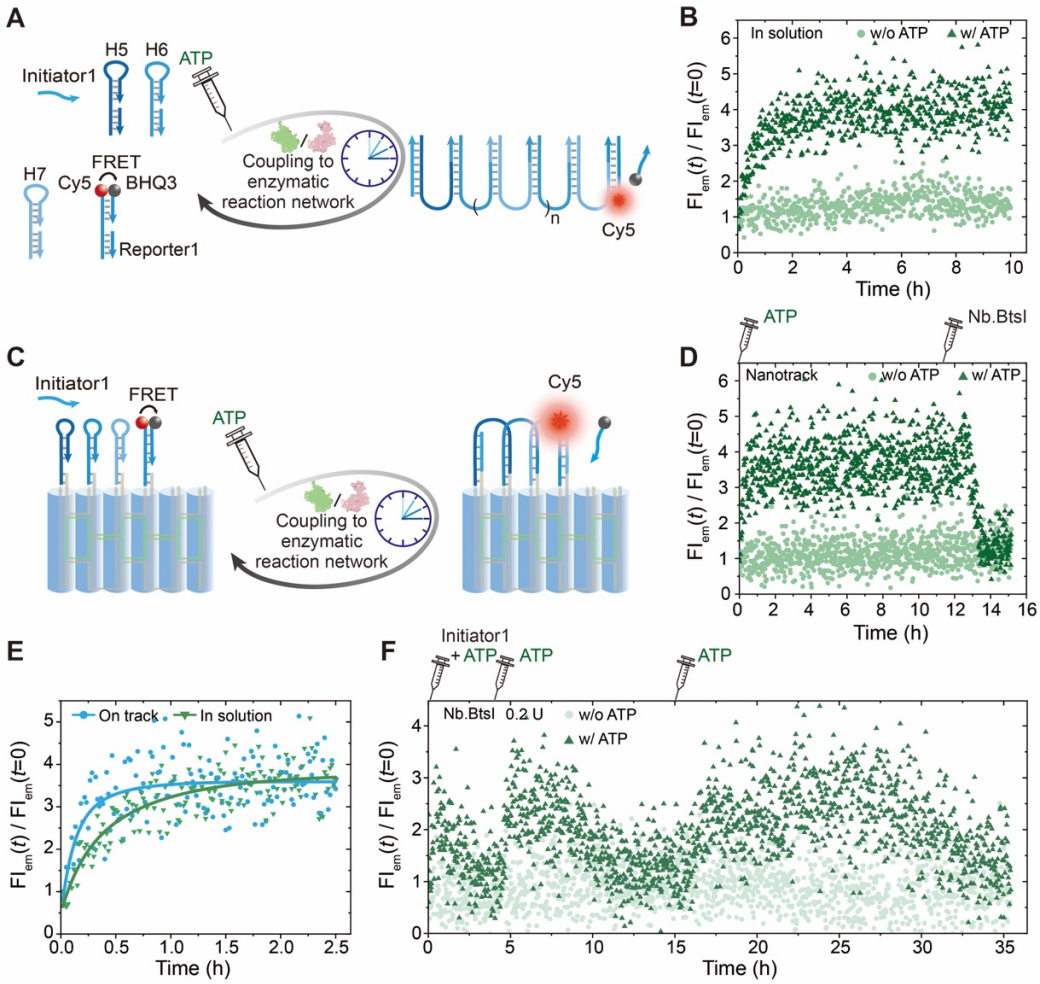


**Supplementary Fig. 14. Fuel-driven transient directional signal transduction on a four-station nanostructure track.** (A) Schematic diagram depicting ATP-fueled signal transduction occurring in solution. (B) Time-dependent FI measurements of fuel-driven signal transduction by cHCR in solution. (C) Schematic illustration of fuel-driven transient signal transduction on a four-station DNA-nanostructure track. (D) Time-dependent FI measurements of fuel-driven signal transduction by cHCR on a four-station DNA-nanostructure track. After the addition of 1 U $\mu L^{-1}$ Nb.BtsI, the system was completely reset after approximately 2 h. (E) Comparison of the signal transduction efficiency between ATP-fueled directional signal transduction on a four-station DNA-nanostructure track and ATP-fueled signal transduction without nanotrack confinement. (F) Time-dependent FI measurements of fuel-driven transient signal transduction with multiple rounds of ATP fueling. Conditions: (B) 37 °C, 180 nM initiator, 18 nM each hairpin monomer, 40 U $\mu L^{-1}$ T4 DNA ligase, and 5 μM ATP. (D) the same as (B) except that a four-station DNA-nanostructure track was used. (F) 37 °C, 18 nM four-station DNA-nanostructure track supplemented with 180 nM quencher strand, 80 U $\mu L^{-1}$ T4 DNA ligase, 0.2 U $\mu L^{-1}$ Nb.BtsI. Repeated fueling of the system with 200, 500, and 900 nM ATP. Red and black balls in the schemes represent Cy5 and dye quencher, respectively. The experiments in Supplementary Fig. 14B, D, E, and F were independently repeated three times with similar results. Source data are provided as a Source Data file.

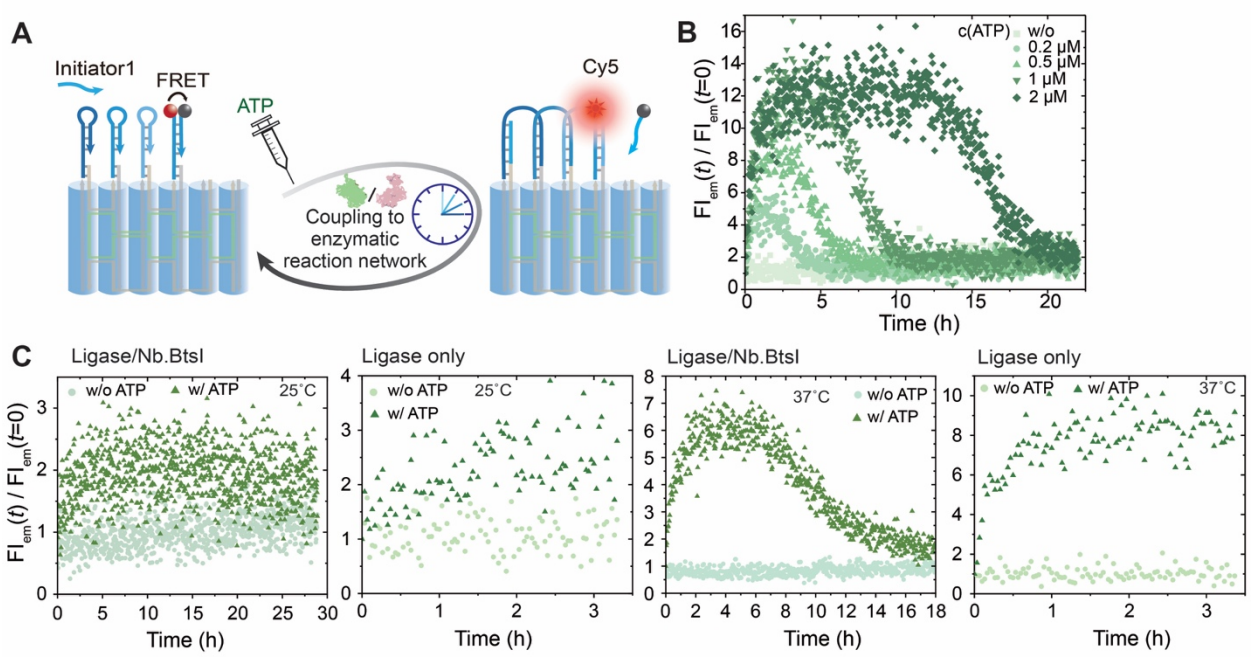


**Supplementary Fig. 15. Fuel-driven directional signal transduction on a four-station nanostructure track.** (A) Schematic illustration of fuel-driven transient signal transduction on a four-station DNA-nanostructure track. (B) Programmable lifetimes of fuel-driven transient signal transduction on a DNA-nanostructure track seen by time-dependent FIs at varied concentration of ATP. (C) Time-dependent FI measurements of ATP-driven directional signal transduction via cHCR on a DNA nanostructure track at 25 and 37 °C, in the presence and absence of Nb.BtsI. Conditions: (B) 1× *NEB* rCutSmart buffer, 37 °C, 500 nM initiator, 50 nM four-station DNA-nanostructure tracks supplemented with 500 nM BHQ3-modified DNA strands, 80 U $\mu L^{-1}$ T4 DNA ligase, 0.1 U $\mu L^{-1}$ Nb.BtsI and and varied concentration of ATP (0, 0.2, 0.5, 1 and 2 μM). (C) 1× *NEB* rCutSmart buffer, 25 or 37 °C, 50 nM four-station DNA-nanostructure tracks supplemented with 500 nM BHQ3-modified DNA strands, 500 nM initiator, 80 U $\mu L^{-1}$ T4 DNA ligase, 1 μM ATP, and in the presence or absence of 0.1 U $\mu L^{-1}$ Nb.BtsI. Red and black balls in the scheme represent Cy5 and dye quencher, respectively. The experiments in Supplementary Fig. 15B and C were independently repeated three times with similar results. Source data are provided as a Source Data file.

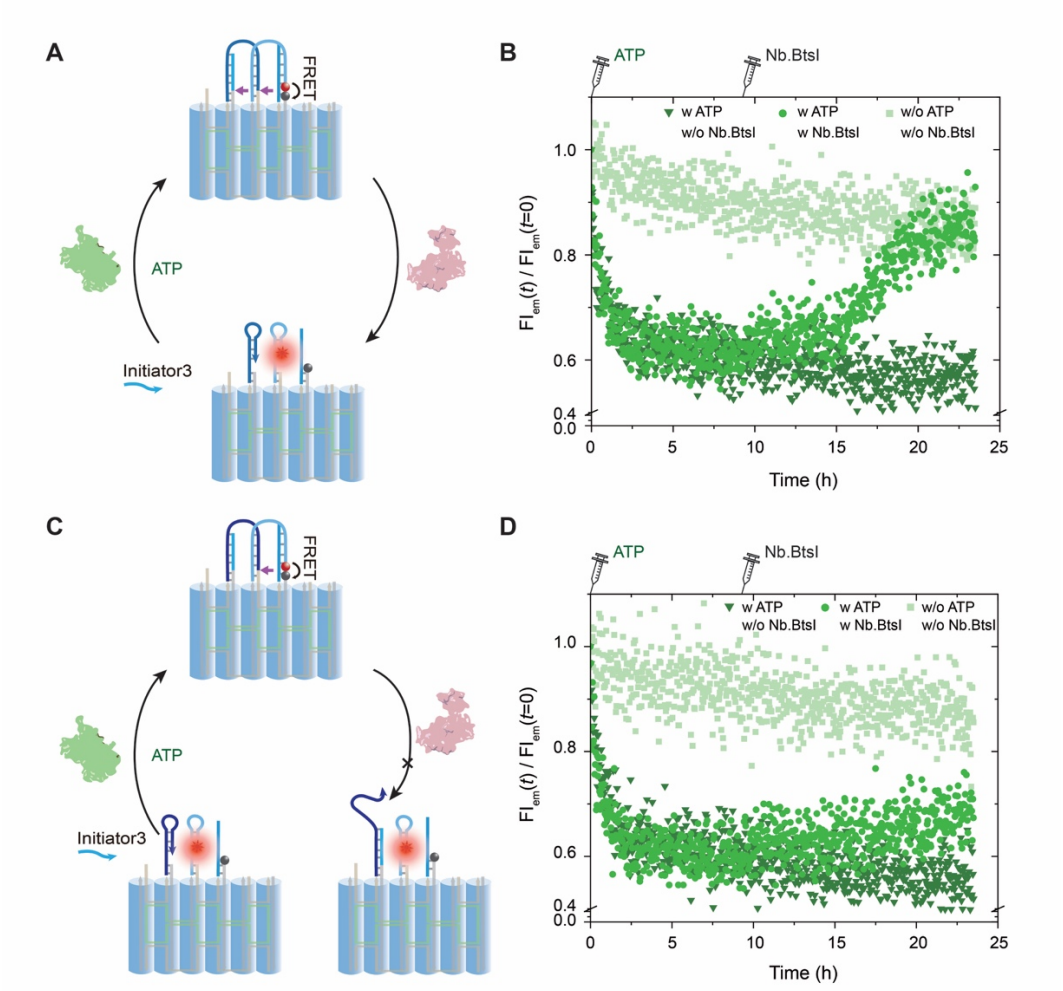


**Supplementary Fig. 16. DNA-nanostructure track resetting mechanism.** (A) Schematic illustration of ATP-fueled directional signal transduction on a three-station DNA-nanostructure track, featuring an initiator cleavable by Nb.BtsI. (B) Time-dependent FI measurements of ATP-fueled directional signal transduction in the presence and absence of post-addition of 0.2 U $\mu L^{-1}$ Nb.BtsI. (C) Schematic illustration of ATP-fueled directional signal transduction on a three-station DNA-nanostructure track, with an initiator uncleavable by Nb.BtsI after ligation. (D) Time-dependent FI measurements of ATP-fueled directional signal transduction in the presence and absence of post-addition of 0.2 U $\mu L^{-1}$ Nb.BtsI. The results indicate that after adding Nb.BtsI to the system containing uncleavable ligated initiator, the FI remains largely constant and does not return to its initial value, revealing the relatively stable nature of the nicked intermediate product. Furthermore, the FI recovery observed upon Nb.BtsI addition in the system with the cleavable initiator indicates that cleavage of the receptor hairpin releases the initiator, enabling hairpin refolding and subsequent sequential refolding of downstream hairpins. This uncovers an additional resetting mechanism for the DNA-nanostructure track beyond the terminal monomer refolding and shedding pathway. Conditions: 1× *NEB* rCutSmart buffer, 37 °C, 50 nM three-station DNA-nanostructure tracks, 500 nM initiator, 80 U $\mu L^{-1}$ T4 DNA ligase, 0. 2 U $\mu L^{-1}$ Nb.BtsI, and 500 nM ATP. Red and black balls in the schemes represent Cy5 and dye quencher, respectively. The experiments in Supplementary Fig. 16B and D were independently repeated three times with similar results. Source data are provided as a Source Data file.

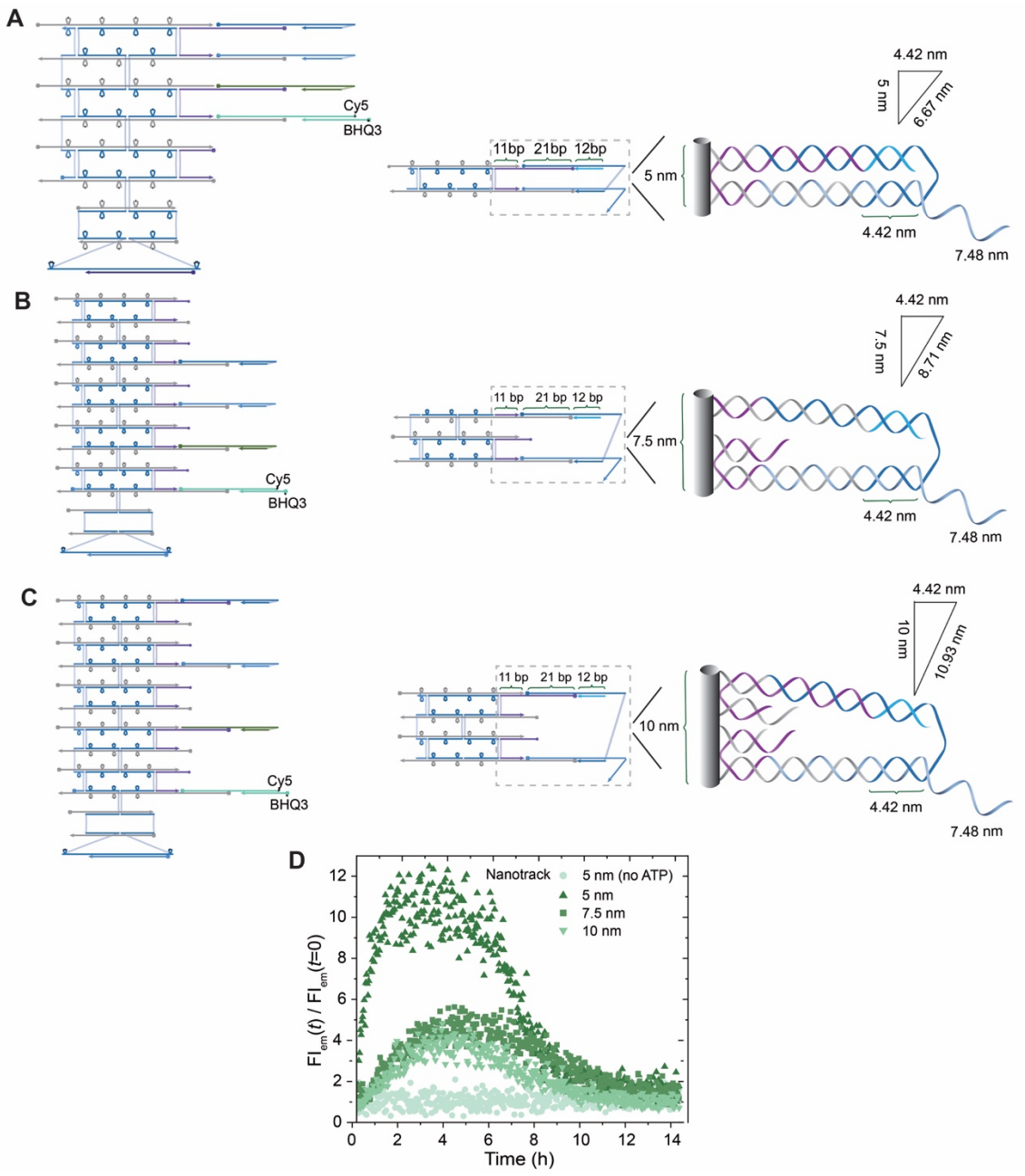


**Supplementary Fig. 17. Fuel-driven transient directional signal transduction on a four-station nanostructure track with varied inter-hairpin distance.** (A–C) Designs of four-station DNA-nanostructure tracks with inter-hairpin distances of (A) 5 nm, (B) 7.5 nm, and (C) 10 nm, including the calculation of the theoretical length of the opened hairpin portion required for effective ligation with the adjacent hairpin. (D) Time-dependent FI measurements of fuel-driven signal transduction on four-station DNA-nanostructure tracks with different inter-hairpin distances. Conditions: 1× *NEB* rCutSmart buffer, 37 °C, 50 nM four-station DNA-nanostructure tracks supplemented with 500 nM BHQ3-modified DNA strands, 500 nM initiator, 80 U $\mu L^{-1}$ T4 DNA ligase, 0.1 U $\mu L^{-1}$ Nb.BtsI and 1 μM ATP. The experiments in Supplementary Fig. 17D were independently repeated three times with similar results. Source data are provided as a Source Data file.

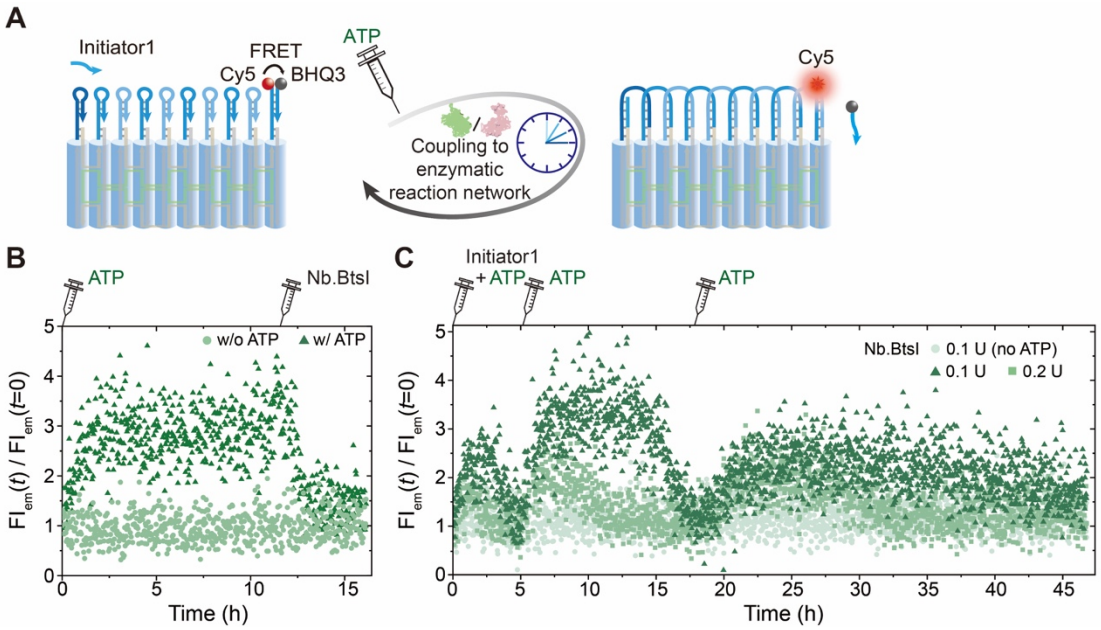


**Supplementary Fig. 18. Fuel-driven transient directional signal transduction on a ten-station nanostructure track.** (A) Schematic illustration of fuel-driven transient signal transduction on a ten-station DNA-nanostructure track. (B) Time-dependent FI measurements of fuel-driven signal transduction by cHCR on a ten-station DNA-nanostructure track. After the addition of 1 U $\mu L^{-1}$ Nb.BtsI, the system was completely reset after approximately 2 h. (C) Time-dependent FI measurements of fuel-driven transient signal transduction with multiple rounds of ATP fueling. Conditions: (B) 37 °C, 24 nM ten-station DNA-nanostructure track supplemented with 240 nM quencher strand, 40 U $\mu L^{-1}$ T4 DNA ligase, and 5 μM ATP. (C) 37 °C, 18 nM ten-station DNA nanostructure track supplemented with 180 nM quencher strand, 80 U $\mu L^{-1}$ T4 DNA ligase, and varied concentration of Nb.BtsI (0.1, and 0.2 U $\mu L^{-1}$). Repeated fueling of the system with 200, 500, and 900 nM ATP. Red and black balls in the schemes represent Cy5 and dye quencher, respectively. The experiments in Supplementary Fig. 18B and C were independently repeated three times with similar results. Source data are provided as a Source Data file.

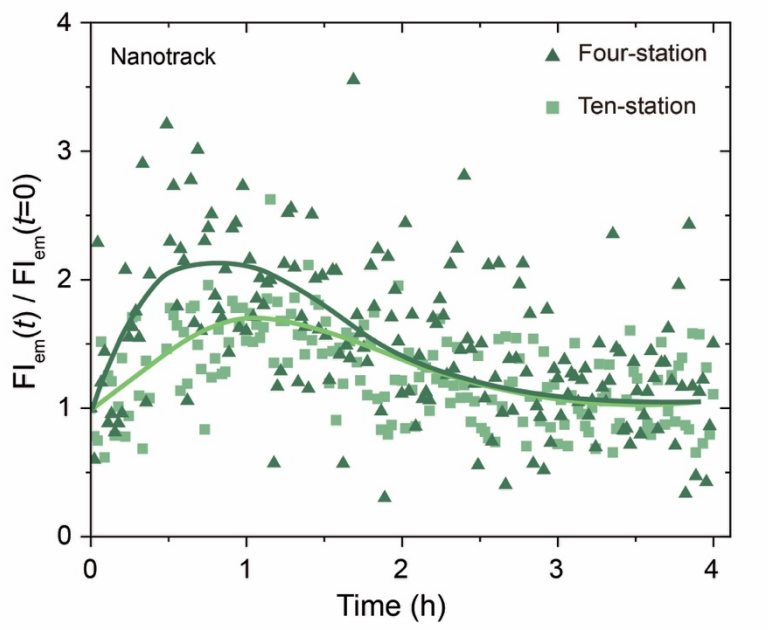


**Supplementary Fig. 19. Fuel-driven transient directional signal transduction on DNA-nanostructure tracks with different distances (i.e. four- and ten-station nanotracks).** The plotted data correspond to the first 4 h period shown in Supplementary Fig. 14F and 18C. Signal transduction covers the full distance of a four-station nanotrack in approximately 0.5 hours, whereas the time required for a ten-station nanotrack is roughly twice as long. Lines are guides to the eye. Conditions: 1× *NEB* rCutSmart buffer, 37 °C, 180 nM initiator, 18 nM DNA-nanostructure tracks supplemented with 180 nM BHQ3-modified DNA strands, 80 U $\mu L^{-1}$ T4 DNA ligase, 0.2 U $\mu L^{-1}$ Nb.BtsI and 200 nM ATP. Source data are provided as a Source Data file.

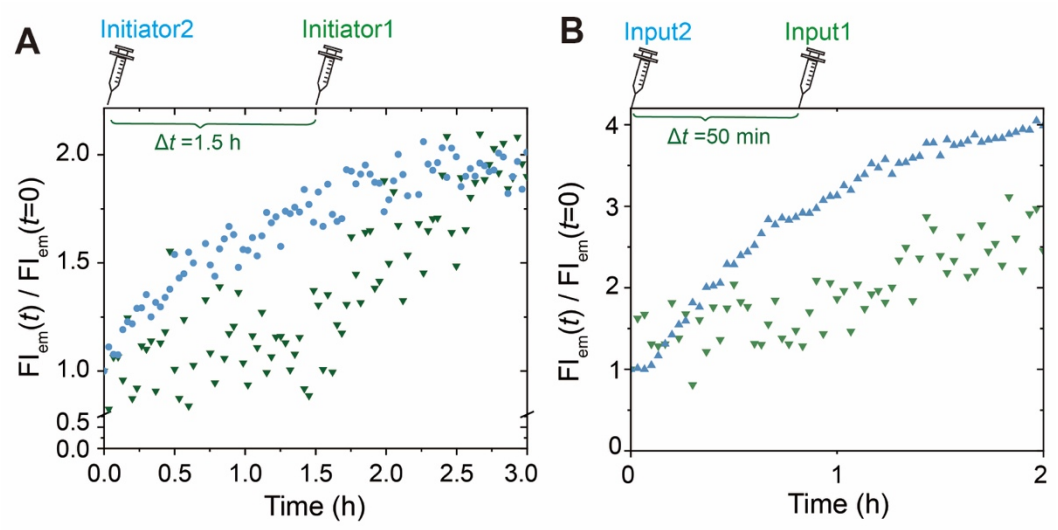


**Supplementary Fig. 20. Time-dependent FI measurements of pathway-selective transient signal transduction.** (A) The plotted data correspond to the first 3 h period shown in Fig. 4I in the main manuscript. (B) The plotted data correspond to the first 2 h period shown in Fig. 5B in the main manuscript. Source data are provided as a Source Data file.

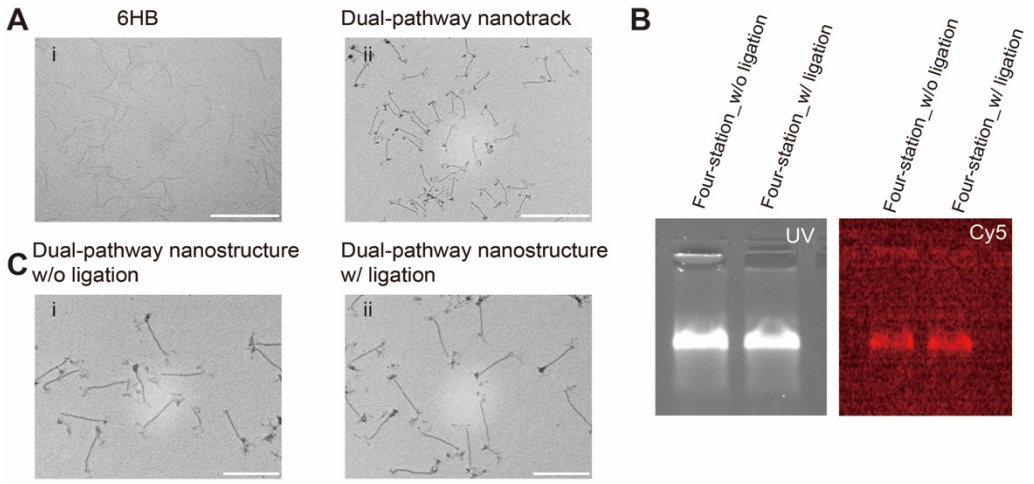


**Supplementary Fig. 21. TEM images of the dual-pathway DNA nanostructure track before and after folding.** (A) TEM images of the (i) 6HB and (ii) dual-pathway DNA-nanostructure. Scale bars: 500 nm. (B) AGE analysis of the directional signal transduction on a four-station DNA-nanostructure track (1 wt. %, 70 V, 1 h), which shows no band shift after ligation, verifying that signal transduction occurs within an individual nanostructure rather than through crosstalk between multiple assemblies. (C) TEM images of the directional transient signal transduction without (i) and with (ii) ligation. Scale bars: 200 nm. The experiments in Supplementary Fig. 21A–C were independently repeated three times with similar results.

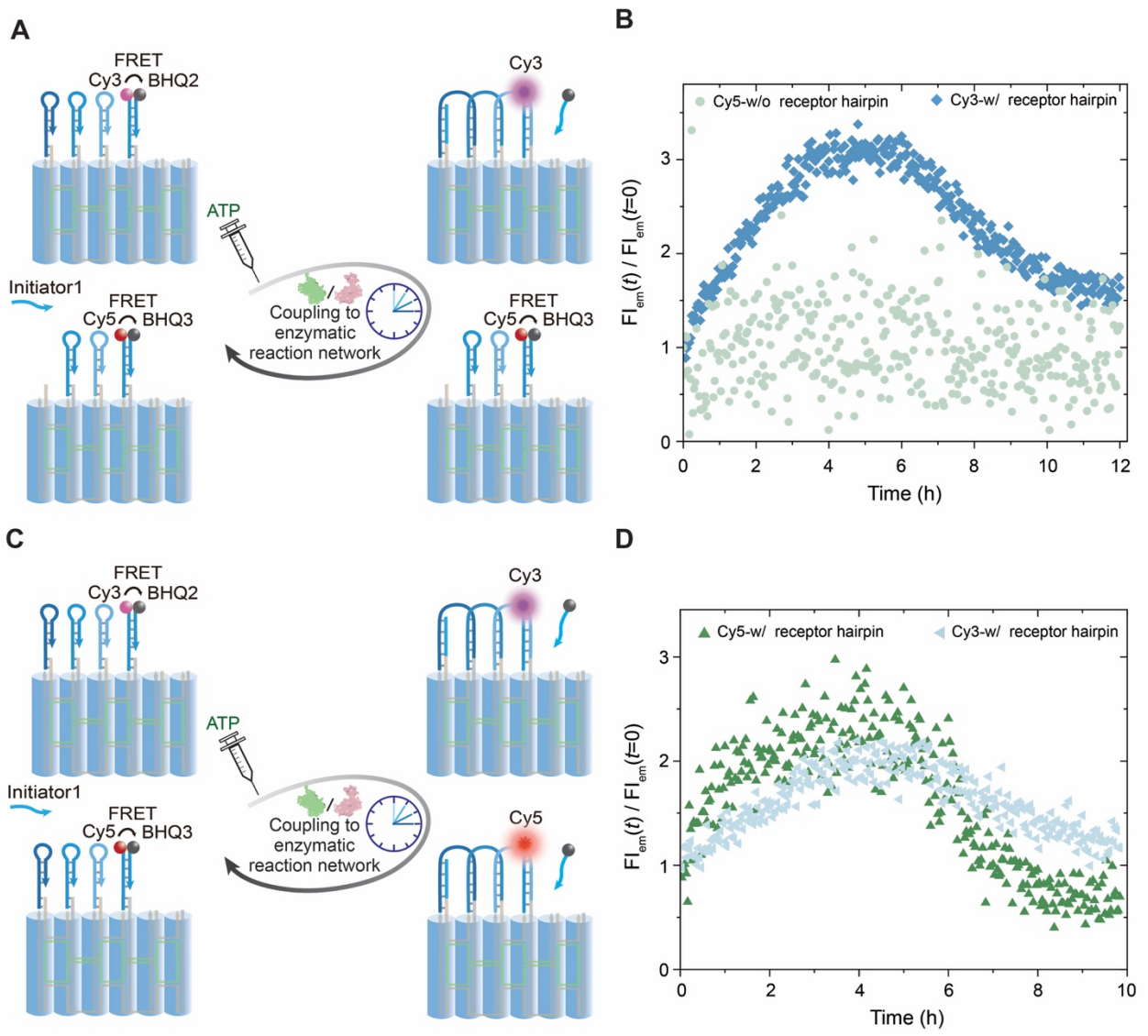


**Supplementary Fig. 22. Evaluation of cross-interaction among DNA-nanostructure tracks via Förster resonance energy transfer (FRET).** (A) Schematic diagram depicting fuel-driven signal transduction on DNA-nanostructure tracks bearing distinct FRET reporters, in the presence and absence of the receptor hairpin. (B) Time-dependent FI measurements of fuel-driven signal transduction on DNA-nanostructure tracks in (A). (C) Schematic diagram depicting fuel-driven signal transduction DNA-nanostructure tracks bearing distinct FRET reporters, both equipped with the same receptor hairpin. (D) Time-dependent FI measurements of fuel-driven signal transduction on DNA-nanostructure tracks in (C). Conditions: 1× *NEB* rCutSmart buffer, 37 °C, 500 nM initiator, 50 nM each DNA-nanostructure tracks supplemented with 500 nM each quencher strand, 80 U $\mu L^{-1}$ T4 DNA ligase, 0.1 U $\mu L^{-1}$ Nb.BtsI and 1 μM ATP. Red, magenta, and black balls in the schemes represent Cy5, Cy3, and dye quencher, respectively. The experiments in Supplementary Fig. 22B and D were independently repeated three times with similar results. Source data are provided as a Source Data file.

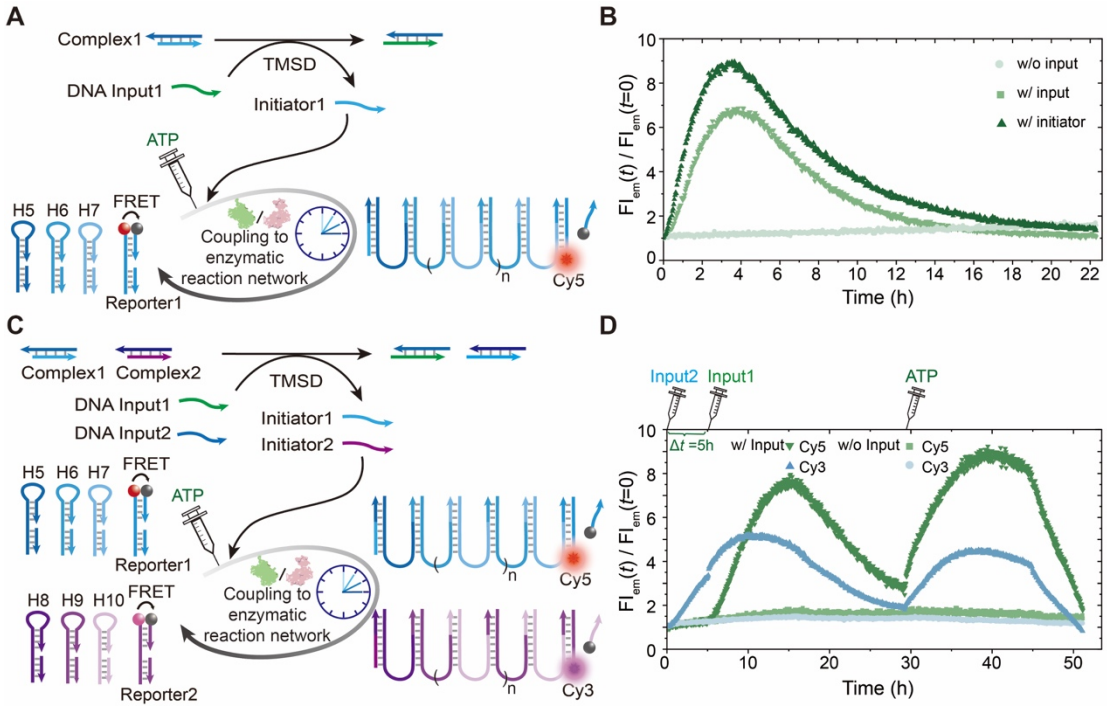


**Supplementary Fig. 23. ATP-fueled transient signaling without nanotrack confinement.** (A) Schematic diagram of ATP-fueled transient signal transduction of Input1. (B) Time-dependent FI measurements of ATP-fueled transient signal transduction. (C) Schematic diagram of ATP-fueled transient transduction of multiple input signals. (D) Time-dependent FI measurements of transient signal transduction of both Inputs. Conditions: (B) 37 °C, 1 μM each hairpin monomer, 1.5 μM Reporter1, 2 μM Complex1, 6 μM DNA Input1, 60 U $\mu L^{-1}$ T4 DNA ligase, 1 U $\mu L^{-1}$ Nb.BtsI, and 4 μM ATP. (D) 37 °C, 1 μM each hairpin monomer, 1.5 μM Reporter1, 1.5 μM Reporter2, 2 μM Complex1, 2 μM Complex2, 6 μM Input1, 6 μM Input2, 80 U $\mu L^{-1}$ T4 DNA ligase, 1 U $\mu L^{-1}$ Nb.BtsI. Repeated fueling of the system with 10, and 6 μM ATP. Red, magenta, and black balls in the schemes represent Cy5, Cy3, and dye quencher, respectively. The experiments in Supplementary Fig. 23B and D were independently repeated three times with similar results. Source data are provided as a Source Data file.

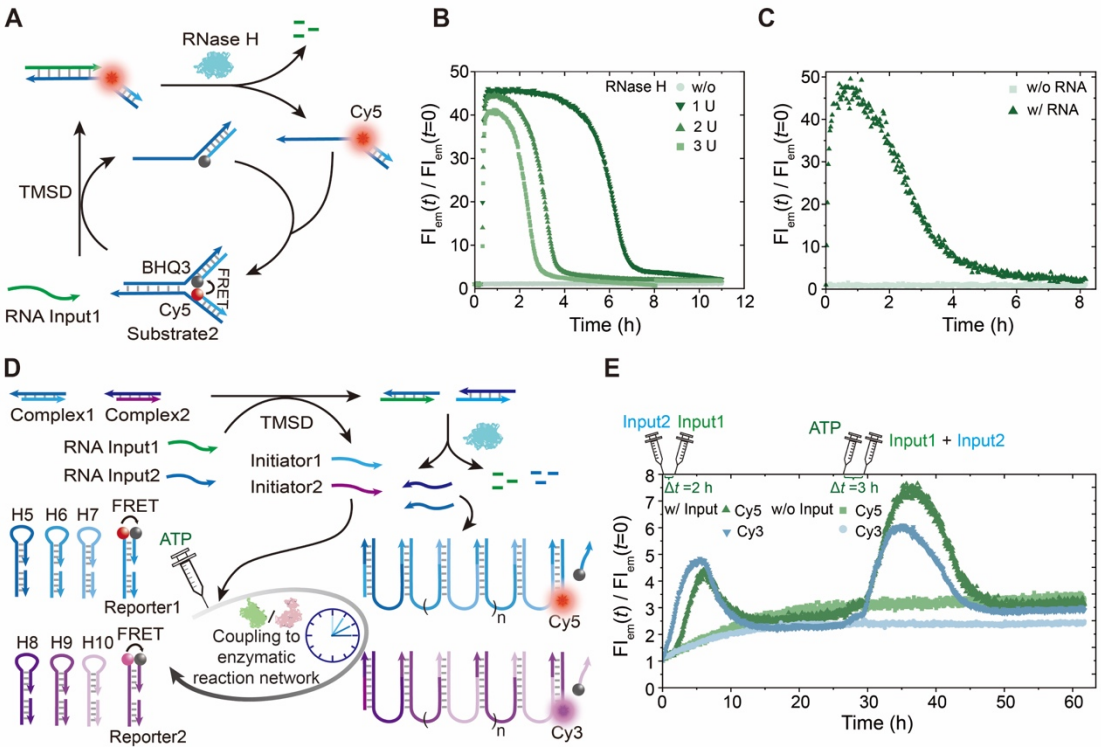


**Supplementary Fig. 24. Autonomous input signal clearance for repeated fuel-driven transient signal transduction without nanotrack confinement.** (A) Schematic diagram of RNA/RNase H reaction network. (B) Time-dependent FI measurements of transient strand displacement using RNA Input at varied concentration of RNase H. (C) Time-dependent FI measurements of transient strand displacement with and without RNA Input. (D) Schematic diagram of autonomous input signal clearance in fuel-driven transient signal transduction. (E) Time-dependent FI measurements of repeated activation of pathway-selective transient signal transduction with autonomous input signal clearance. Conditions: (B) 37 °C, 15 μM RNA Input1, 1 μM Substrate2, and varied concentration of RNase H (1, 2, and 3 U $\mu L^{-1}$). (C) 37 °C, 10 μM RNA Input1, 50 nM Substrate2, and 2 U $\mu L^{-1}$ RNase H. (E) 37 °C, 1 μM each hairpin monomer, 1.5 μM Report1, 1.5 μM Report2, 5 μM Complex1, 5 μM Complex2, 10 μM Input1, 10 μM Input2, 80 U $\mu L^{-1}$ T4 DNA ligase, 1.5 U $\mu L^{-1}$ Nb.BtsI, and 2 U $\mu L^{-1}$ RNase H. Repeated fueling of the system with 10, and 15 μM ATP. Red, magenta, and black balls in the schemes represent Cy5, Cy3, and dye quencher, respectively. The experiments in Supplementary Fig. 24B, C, and E were independently repeated three times with similar results. Source data are provided as a Source Data file.

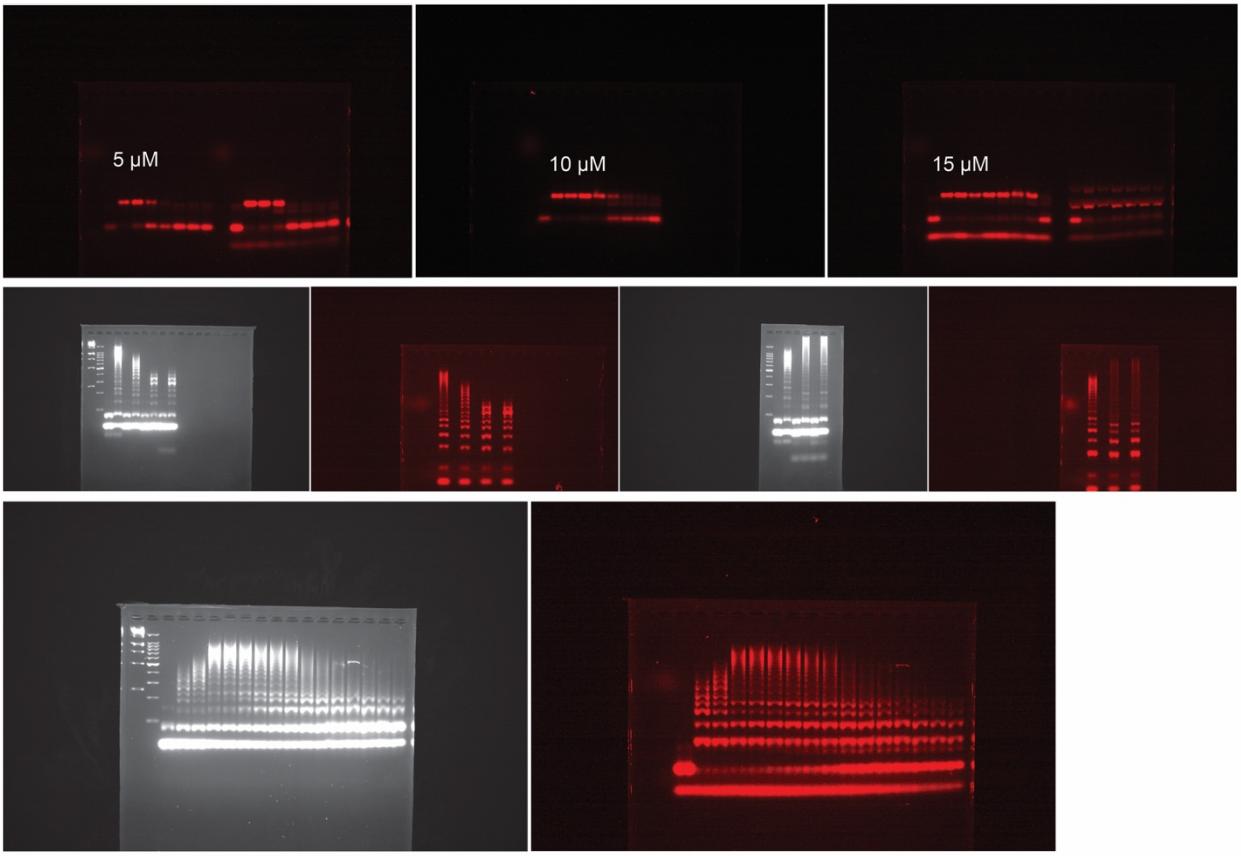


**Supplementary Fig. 25.** Uncropped gel scans for the presented gel images in Fig. 2 in main manuscript.

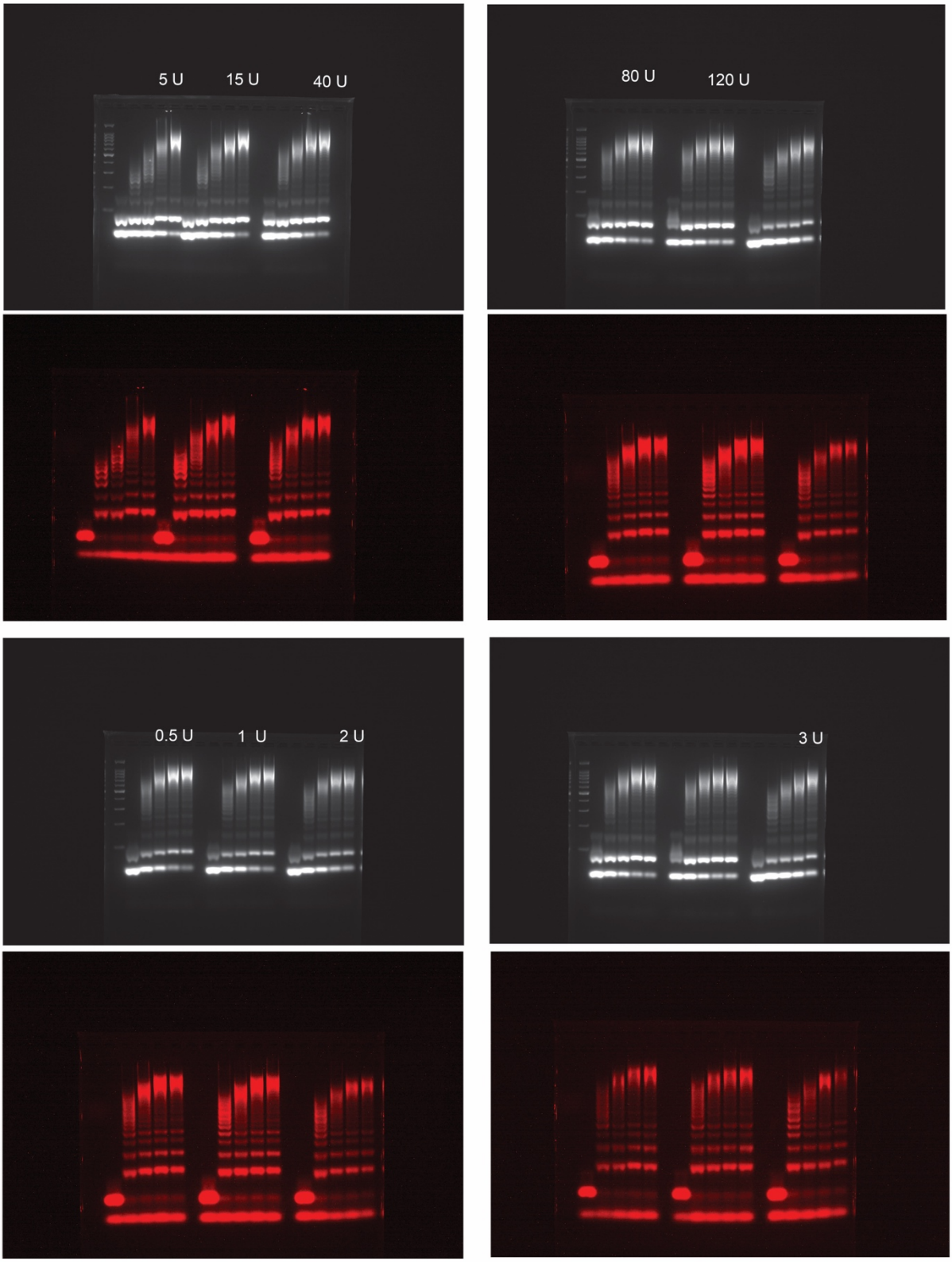


**Supplementary Fig. 26.** Uncropped gel scans for the presented gel images in Supplementary Fig. 4.

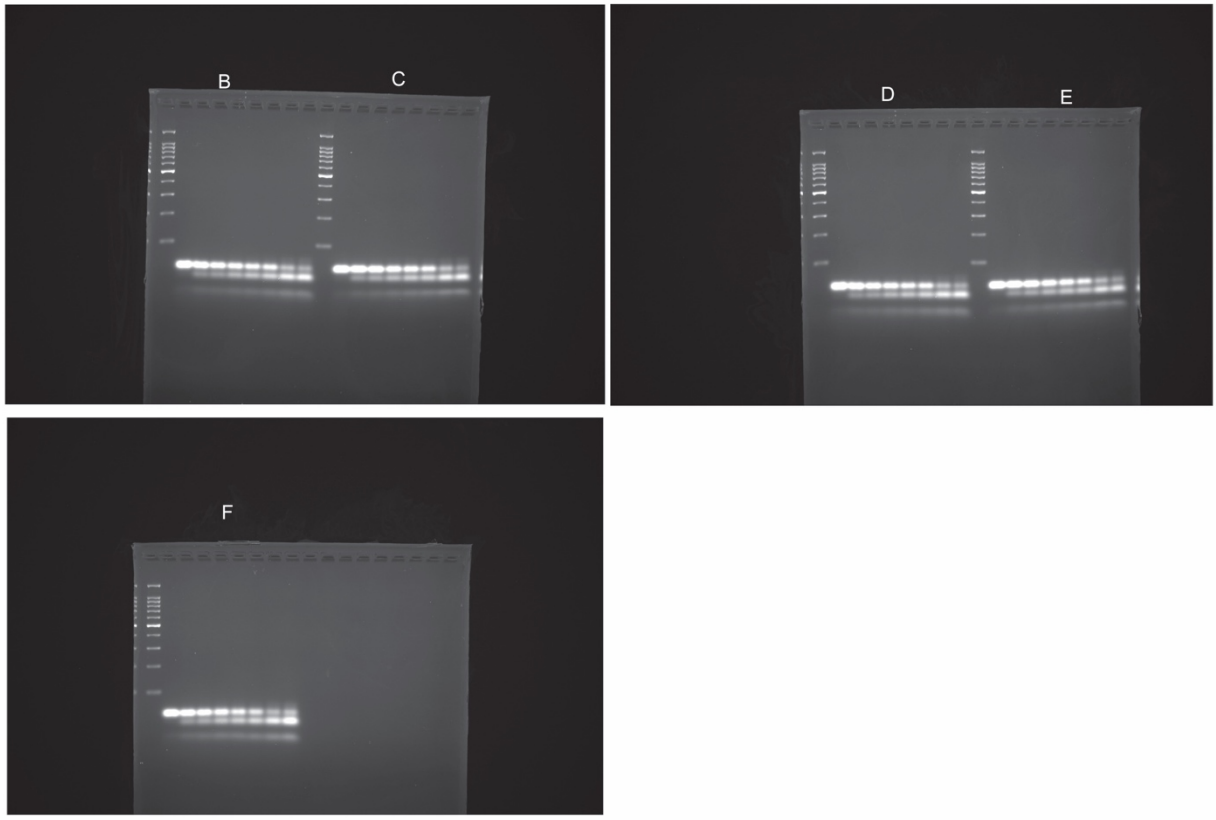


**Supplementary Fig. 27.** Uncropped gel scans for the presented gel images in Supplementary Fig. 7.

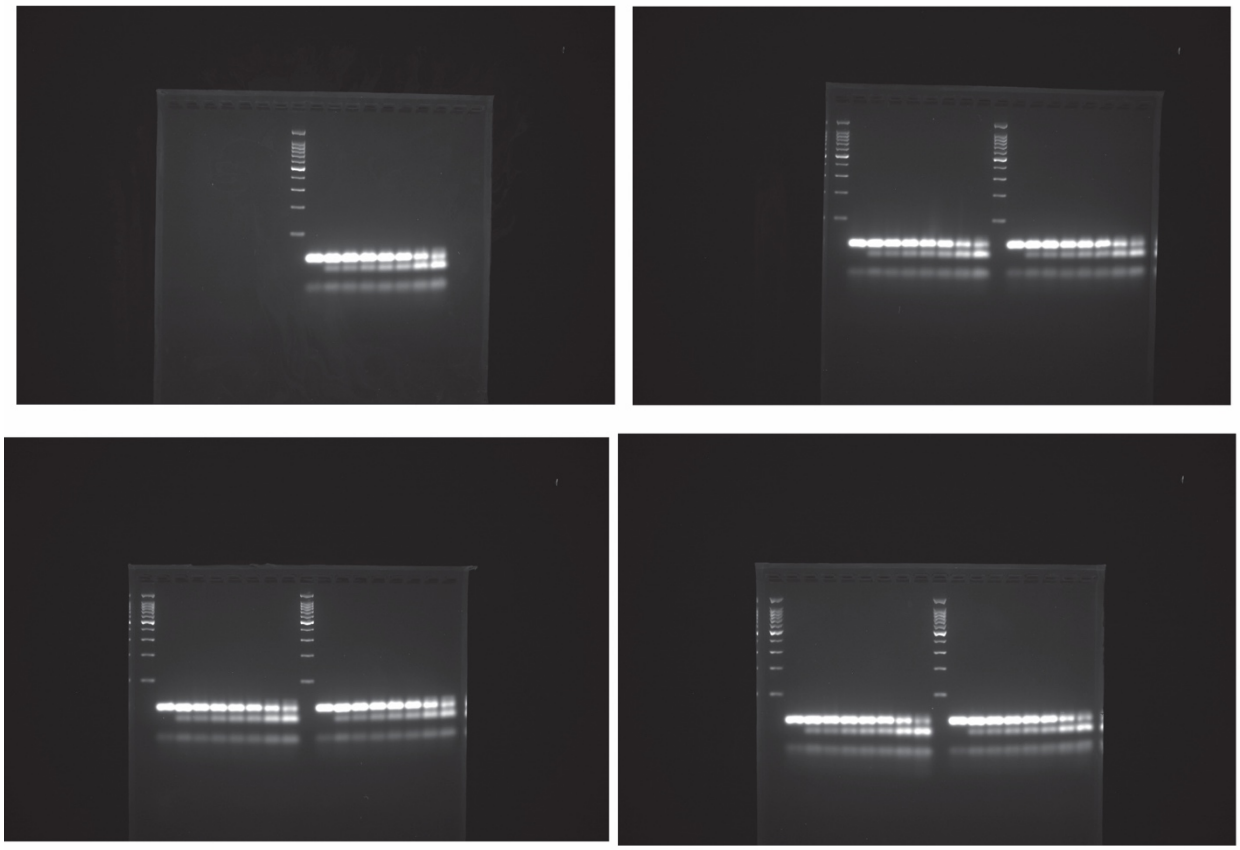

**Supplementary Fig. 28.** Uncropped gel scans for the presented gel images in Supplementary Fig. 8.

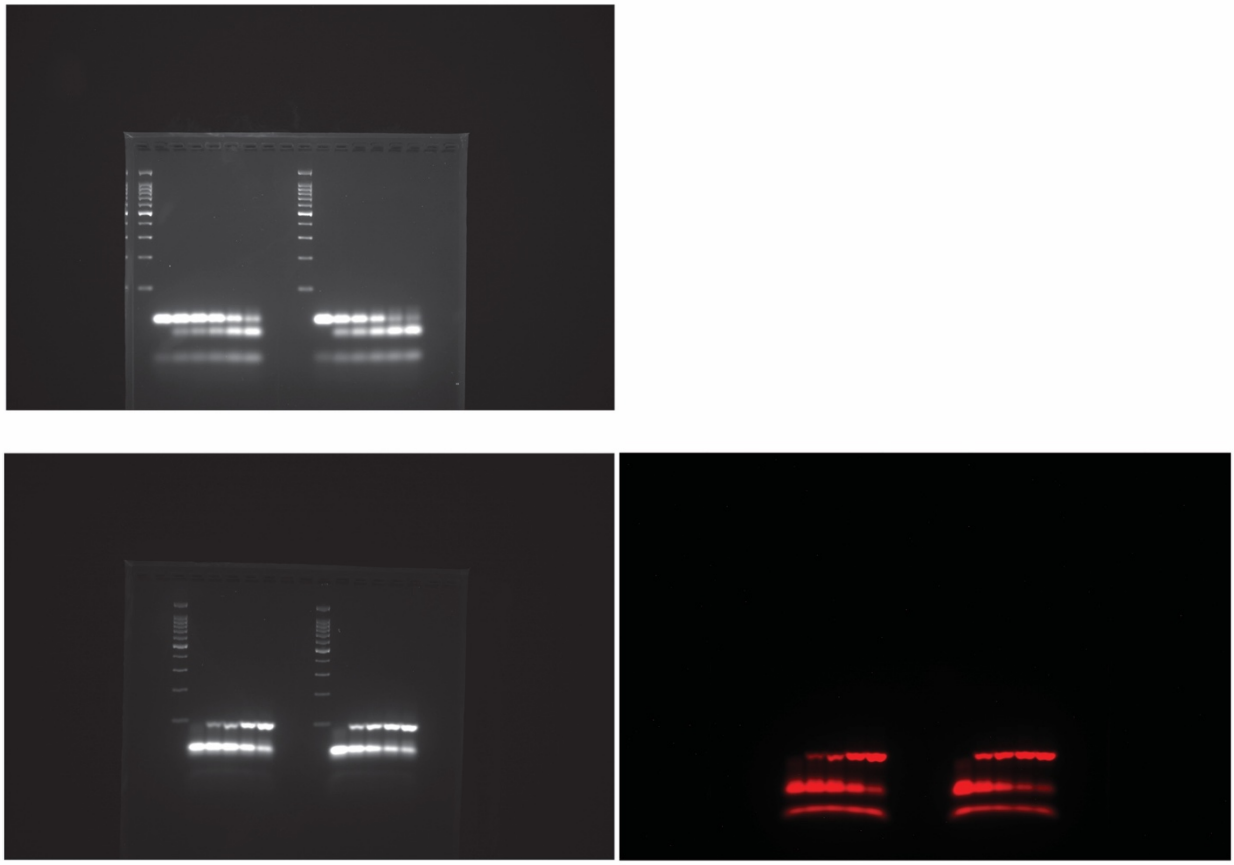

**Supplementary Fig. 29.** Uncropped gel scans for the presented gel images in Supplementary Fig. 9.

**Supplementary Note1**

Because the degradation of DNA polymers proceeds through a terminal monomer shedding mechanism, the lifetime of the ATP-fueled transient cHCR is governed by both the ATP concentration, and the kinetics of monomer refolding and shedding (Supplementary Fig. 5 and 6). This contrasts with the ATP-fueled transient hairpin opening, whose lifetime is dictated primarily by ATP concentration (Supplementary Fig. 1). This is seen by the AGE analyses of time-dependent aliquots of ATP-fueled transient hairpin opening and transient cHCRs. For the ATP-fueled transient hairpin-opening reaction performed at 25 °C in 1× *NEB* rCutSmart buffer containing 1 μM initiator, 2 μM hairpin, 40 U $\mu L^{-1}$ T4 DNA ligase, and 1 U $\mu L^{-1}$ Nb.BtsI, increasing the ATP concentration from 5 to 15 μM extends the system lifetime from ca. 4 to 18 h. In contrast, for the ATP-fueled transient cHCR performed at 25 °C in 1× *NEB* rCutSmart buffer containing 1 μM initiator, 10 μM of each hairpin monomer, 80 U $\mu L^{-1}$ T4 DNA ligase, and 3 U $\mu L^{-1}$ Nb.BtsI—conditions that provide more frequent bond ligation and cleavage and therefore faster ATP consumption—the system lifetime still lasts 1–3 days when fueled with 10 or 20 μM ATP. This lifetime is markedly longer than that observed for the ATP-fueled transient hairpin-opening reaction at comparable fuel levels. Thus, the prolonged lifetime of the transient cHCR must be attributed to the slow terminal monomer shedding process during DNA polymer degradation.